

THREE PROBLEMS IN NONLINEAR DYNAMICS:
TIME DELAY, FRACTIONALITY AND
SYNCHRONIZATION

A Dissertation

Presented to the Faculty of the Graduate School
of Cornell University

in Partial Fulfillment of the Requirements for the Degree of
Doctor of Philosophy

by

Meghan Kathleen Suchorsky

January 2012

© 2012 Meghan Kathleen Suchorsky
ALL RIGHTS RESERVED

THREE PROBLEMS IN NONLINEAR DYNAMICS: TIME DELAY,
FRACTIONALITY AND SYNCHRONIZATION

Meghan Kathleen Suchorsky, Ph.D.

Cornell University 2012

Three problems in nonlinear dynamics are studied with concern to the effects of time history dependent functions on steady state behavior. In each problem we consider either a single oscillator or a system of oscillators. The appearance of the time history dependence varies over the problems, and is be introduced either as a delayed term or a fractional derivative.

In our first problem, a van der Pol type system with delayed feedback is explored by employing a two variable expansion perturbation method. The resulting amplitude-delay relation predicts two Hopf bifurcation curves, such that in the region between these two curves oscillations will be quenched. The perturbation results are verified by comparison with numerical integration.

The second and third problems are on the subject of fractional derivatives. In analyzing these problems we look to extend classic perturbation methods to the treatment of fractional derivatives.

In the second problem we also consider a single oscillator. The oscillator may be described as a damped Mathieu type where the damping term has been replaced by a fractional derivative. The order of the fractional derivative considered ranges from 0 to 1. Both lowest order and higher order approximations for the $n = 1$

transition curves, which separate regions of stability from instability, are found using the method of harmonic balance. An approximation for the $n = 0$ transition curve is also obtained. In the limiting cases of the fractional derivative's order, α , being 0 or 1, the fractional Mathieu equation being considered respectively reduces to the familiar undamped and damped Mathieu equations. The undamped and damped Mathieu equations are well studied and our results may be compared with the known results in these cases. Through these comparisons conclusions are drawn as to the validity of assumptions made in applying the method of harmonic balance as well as the effect of the fractional derivative.

In the third problem, the stability of the in-phase and out-of-phase modes of a pair of fractionally-coupled van der Pol oscillators is studied. A two variable perturbation method is applied to the system's corresponding variational equations to obtain expressions for the transition curves separating regions of stability from instability. The perturbation results are validated with numerics and, as in the second problem, through direct comparison with known results in the limiting cases of fractional derivative order taking on the values of $\alpha = 0$ and $\alpha = 1$.

BIOGRAPHICAL SKETCH

Meghan Kathleen Suchorsky was born on March 27, 1983 in Somerville, New Jersey. She graduated from Hunterdon Central Regional High School in Flemington, NJ in 2001, received her Bachelor of Science degree in Mechanical Engineering from Rutgers University in May 2006 and her Master of Science in Theoretical and Applied Mechanics from Cornell University in January 2009.

ACKNOWLEDGEMENTS

I would like to thank my thesis advisor and committee chair, Richard Rand, for all his support and encouragement. I would also like to thank Alan Zehnder and Steven Strogatz for serving on my committee.

I would like to acknowledge and thank my coauthor Si Mohamed Sah, [33], [43], as well as Duane Storti for a helpful discussion.

Lastly I would like to thank my family for their love and support.

TABLE OF CONTENTS

Biographical Sketch	iii
Acknowledgements	iv
Table of Contents	v
List of Figures	vii
1 Outline of the Thesis	1
2 Differential Delay Equations	5
2.1 The Initial-Value Problem	5
2.2 Method of Steps	7
2.3 The Characteristic Equation	9
3 The van der Pol Oscillator under Delayed Feedback [43]	14
3.1 Introduction	14
3.2 Perturbation analysis	16
3.2.1 Simple harmonic oscillator with delayed feedback	16
3.2.2 Two variable expansion method	19
3.2.3 Stability of the limit cycle	25
3.3 Hopf bifurcation	28
3.3.1 Predicted Hopf bifurcation surface	28
3.3.2 Discussion: Comparison with Atay [2]	31
3.4 Summary	35
4 The Fractional Calculus	37
4.1 Fractional Derivatives	39
4.2 Several Methods for Solving Fractional Differential Equations	43
4.2.1 Laplace transform approach	44
4.2.2 Power Series Approach	52
4.2.3 Numerical Solution	55
5 Fractional Mathieu Equation [33]	60
5.1 Mathieu's Equation	60
5.2 Transition curves of the fractional Mathieu equation	62
5.3 Discussion	65
5.4 Summary	69
6 A pair of van der Pols coupled with fractional derivatives [44]	70
6.1 Stability of the in-phase mode	71
6.2 Stability of the out-of-phase mode	79
6.3 Summary	89
7 Summary	91

A Matlab and Maxima Scripts	93
A.1 Laplace transform method results of section 4.2.1	93
A.2 Power series method results of section 4.2.2	94
A.3 Numerical integration code of section 4.2.3	95
Bibliography	97

LIST OF FIGURES

2.1	Solutions to (2.7) obtained using the method of steps (solid lines) and numerical integration using dde23 (asterisks). The arrows depict how the method of steps was performed.	9
2.2	Cartoon depicting how an infinite number of characteristic roots emerge when even the smallest amount of delay is added to a system. Specifically our system (2.12) is considered which has only one root when there is no delay since it is first order.	11
2.3	Numerical integration of linear and non-linear equations, at delays before and after the first critical Hopf value of $T = \frac{\pi}{2}$. The top row of the figure show plots of solutions to the linear equation (2.12) before and after the Hopf value and we see that the stability of the origin has changed but no limit cycle is created as the equation has no nonlinear terms. The second row of plots again shows the solution to the nonlinear equation (2.19) before and after the Hopf value where now a stable limit cycle has been born in the bifurcation.	13
3.1	Surface plot of ω as a function of β and δ , as given by (3.8), with chosen parameters $\gamma = 1, \alpha = 1$	30
3.2	Surface plot of the critical delay lag T_{cr} necessary for a Hopf bifurcation as a function of β and δ , as given by (3.59), with chosen parameters $\gamma = 1, \alpha = 1, \epsilon = 0.1$	31
3.3	Three different cuts of the Hopf surface of Fig.3.2, defined by (3.59), where $\gamma = 1, \alpha = 1, \epsilon = 0.1$. Figure (a) shows the Hopf curve produced by cutting the Hopf surface at $\beta = 0$. Similarly (b) and (c) show the Hopf curves for $\delta = 0$ and $\beta = \delta$ respectively.	32
3.4	Cut at $\beta = 0$ of Hopf surface, Fig.3.2, defined by (3.59). The transition from a region of oscillation (a), to no oscillation (b), and back to oscillation (c), as the Hopf curves are crossed, for $\gamma = 1, \alpha = 1, \epsilon = 0.1$ is shown. Displayed is x versus t obtained by numerical integration of eq.(3.2).	32
3.5	Cut at $\delta = 0$ of Hopf surface, Fig.3.2, given by (3.59). The transition from a region of oscillation (a), to no oscillation (b), and back to oscillation (c), as the Hopf curves are crossed, for $\gamma = 1, \alpha = 1, \epsilon = 0.1$ is shown. Displayed is x versus t obtained by numerical integration of eq.(3.2).	33
3.6	Cut at $\beta = \delta$ of Hopf surface, Fig.3.2, given by (3.59). The transition from a region of oscillation (a), to no oscillation (b), and back to oscillation (c), as the Hopf curves are crossed, for $\gamma = 1, \delta = 1, \epsilon = 0.1$ is shown. Displayed is x versus t obtained by numerical integration of eq.(3.2).	33

3.7	Plot of T_{cr} vs. ϵ , as given by (3.59), where $\beta = \delta = 0.5$. The grey region represents no oscillation, as concluded by numerical integration. Beyond ϵ_{cr} the oscillations may no longer be quenched with delay.	34
3.8	Comparison of our Hopf bifurcation curve, eq.(3.44), vs. Atay's [2], eq.(3.62), which is based on assuming both small delay amplitude and small delay lag. x's represent numerical integration of eq.(3.2). Parameters taken as, $\gamma = 1, \alpha = 1, \beta = 0, \epsilon = 0.1$	35
4.1	Solution to (4.31) with $\mu = 1$ and $\alpha = 1/2$ given by (4.68) with (4.72) found using the Laplace transform method.	52
4.2	Solution to (4.31) given by (4.73) and (4.79) with $\mu = 1, \alpha = 1/2$, and $v = 2$ truncated to approximately 30 non-zero terms.	54
4.3	Comparison of solutions to (4.31) with $\mu = 1$ and $\alpha = 1/2$ predicted using the Laplace transform method and power series method. The Laplace solution given by (4.68) with (4.72) is shown by the solid line. The power series solution is given by (4.73) and (4.79) with $v = 2$ and truncated to approximately 30 non-zero terms and shown by the asterisks.	55
4.4	Solution obtain by numerically integrating (4.31) with $\mu = 1$ and $\alpha = 1/2$	58
4.5	Comparison of numerical solution to (4.31) with $\mu = 1$ and $\alpha = 1/2$, shown as a solid line and solution found using the Laplace transform method shown with asterisks.	59
4.6	Numerical integration of (4.31) with $\mu = 1$ and $\alpha = 1/2$	59
5.1	Transition curves in Mathieu's equation (5.1). Displayed are eqs.(5.3),(5.4) as well as other curves whose equations are not listed here. See [31].	61
5.2	Transition curves (5.6) in the damped Mathieu equation (5.5). The upper curve corresponds to $c = 0.5$. The middle curve corresponds to $c = 0.1$. The lower curve corresponds to $c = 0$	62
5.3	$n = 1$ transition curve, eq.(5.18), in the fractional Mathieu equation (5.7) for $c = 0.1$ and $\alpha = 0, 0.5, 1$	65
5.4	$n=1$ transition curves in the fractional Mathieu equation (5.7) for $\alpha = 0.5$ and $c = 0.1$. First and second order approximations, as obtained by the method of harmonic balance. The first order approximation is given by eq.(5.18). The second order approximation has 51 terms and is too long to list here.	66
5.5	$n = 0$ transition curve, eq.(5.21), in the fractional Mathieu equation (5.7) for $c = 0.1$ and $\alpha = 0, 0.5, 1$. The leftmost curve corresponds to $\alpha = 0$. The middle curve corresponds to $\alpha = 0.5$. The rightmost curve corresponds to $\alpha = 1$	67
5.6	Eq.(5.18) displayed in $\delta - \epsilon - \alpha$ space for $c = 0.1$	68

5.7	Plot of ϵ_{min} , the minimum quantity of forcing amplitude ϵ necessary to produce instability, as a function of fractional derivative order α , eq.(5.22). The greatest effect is observed where this curve achieves its maximum, shown as a dot here, and referred to as α^* in the text.	69
6.1	Stability of the in-phase mode as predicted by the perturbation method. S denotes stable and U unstable. Regions I and III are both stable and composed of nodes and foci. Regions II, IV and V are unstable. Regions II and IV are filled with saddles and region V is composed of unstable nodes and foci, cf. (6.37)-(6.38).	77
6.2	Comparison of perturbation method's stability results for the in-phase mode previously shown in Fig.6.1 with numerical integration of (6.10) with u given by (6.20) and ϵ taken as $\epsilon = .01$. The asterisks represent stable parameter values and the circles unstable.	78
6.3	The perturbation method predicts the out-of-phase mode to exist only in region I as denoted by \exists cf. eq.(6.57). The out-of-phase mode doesn't exist in region II as noted in figure by \nexists symbol.	82
6.4	The perturbation method predicts the out-of-phase motion to be stable in region Ia and unstable in region Ib cf. eq.(6.82). The out-of-phase motion does not exist in region II cf. eq.(6.57). S is stable, U is unstable and \nexists is does not exist.	87
6.5	Comparison of the out-of-phase perturbation method's results with numerical integration of (6.61) with q given by (6.71) and $\epsilon = 0.1$. The asterisks represent stable parameter values and the circles unstable. \nexists represents that the out-of-phase mode does not exist.	88
6.6	Stability results for both the in-phase and out-of-phase modes. In region A the in-phase mode is stable and the out-of phase mode does not exist as denoted by (S, \nexists) . In region B the in-phase mode is stable and the out-of-phase mode is unstable, (S, U) . In region C both the in-phase and out-of-phase modes are stable, (S, S) . In region D the in-phase mode is unstable and the out-of-phase mode is stable, (U, S) . In region E both modes are again stable, (S, S) .	90

CHAPTER 1
OUTLINE OF THE THESIS

In this thesis three problems in nonlinear dynamics are studied to explore the effects of time delay and fractional derivatives on a system's steady state behavior. The introduction of time delay or fractional derivatives into a system creates a dependence on the time history of a function. In all three problems classical perturbation methods are extended to the treatment of these functional type problems.

In our first problem, a van der Pol type system with delayed feedback is considered. Before analyzing the system an introduction to differential delay equations, DDEs, is provided in Chapter 2. This introduction to DDE theory is structured around contrasting ordinary differential equations, ODEs, with DDEs. The subjects of the initial value problem and the characteristic polynomial are of central focus in Chapter 2 as they are of direct importance in our analysis of the delayed van der Pol oscillator of Chapter 3.

In Chapter 3 the van der Pol type system with delayed feedback is explored:

$$\ddot{x} + x - \epsilon\gamma\dot{x} + \epsilon\alpha x^2\dot{x} = \beta\dot{x}(t - T) + \delta x(t - T) \quad (1.1)$$

This work considers the effect of delay on the steady state behavior of a system, namely limit cycle oscillations. A two variable expansion perturbation is employed and is based on choosing a critical value for the delay corresponding to a Hopf bifurcation in the unperturbed $\epsilon = 0$ system. The perturbation method produces an amplitude-delay relation which predicts two Hopf bifurcation curves. In the region between these two Hopf bifurcation curves oscillations will be quenched. The perturbation results are compared with numerical integration and shown to be in good agreement. The assumptions made in applying the two variable perturbation

method to our delayed system are therefore substantiated.

In the second and third problems we move on to the subject of fractional derivatives. An introduction to this subject is given in Chapter 4. The fractional derivative operator is an extension of the familiar integer order derivative to arbitrary order including integer, rational, irrational and complex values. In section 4.1 the Riemann-Liouville integral is derived to represent the fractional derivative. Issues of convergence are ignored and the derivation presented may be considered as more of a plausibility argument than a rigorous derivation. As in our introduction to DDE theory, insight into the nature of solutions to fractional differential equations is gained through comparisons with ODEs. Comparisons are not made directly, instead an example problem, a linear fractional differential equation, is solved using three standard methods of ODE theory. The three methods presented in section 4.2 are the Laplace transform method, positing a power series solution and numerical integration. The additional steps and obstacles that arise in applying these standard methods to fractional equations give the reader some insight into the difficulties of solving fractional differential equations.

In Chapter 5 we look to extend the treatment of Mathieu's equation by studying an oscillator that can be described as a damped Mathieu equation where the damping term has been replaced by a fractional derivative:

$$x'' + (\delta + \epsilon \cos t)x + cD^\alpha x = 0 \tag{1.2}$$

where $D^\alpha x$ is the order α derivative of $x(t)$ and $0 < \alpha < 1$. Mathieu's equation often arises in questions of stability of motion as well as systems that are parametrically excited. In questions of stability the concern is whether solutions are bounded and therefore stable, or unbounded and correspondingly unstable. Tran-

sition curves divide the parameter plane into regions of stability and instability. The transition curves corresponding to the familiar undamped and damped Mathieu equations are reviewed in section 5.1. These known results are valuable in our investigation of the fractional Mathieu equation since in the limiting cases of $\alpha = 0$ or $\alpha = 1$, the fractional Mathieu equation reduces to the undamped Mathieu equation and the damped Mathieu equation respectively. Using the method of harmonic balance, both a lowest order approximation and higher order approximation for the $n = 1$ transition curves are obtained for the fractional Mathieu equation. An approximation for the $n = 0$ transition curve is also obtained. To apply the method of harmonic balance to the fractional differential equation simplifying assumptions were necessary. The found results are compared in the limiting cases of $\alpha = 0$ and $\alpha = 1$ to validate these assumptions as well as to draw conclusions on the effect of the fractional derivative.

In Chapter 6 a pair of van der Pol oscillators coupled by fractional derivatives is investigated:

$$x'' - \epsilon(1 - x^2)x' + x = \epsilon \gamma D^\alpha(y - x) \quad (1.3)$$

$$y'' - \epsilon(1 - y^2)y' + y = \epsilon \gamma D^\alpha(x - y) \quad (1.4)$$

where again we consider $0 < \alpha < 1$. Of interest is the stability of the in-phase and out-of-phase modes. Both modes have a set of variational equations which govern the evolution of a small disturbances from it. The variational equations unsurprisingly are reminiscent of the previously considered fractional Mathieu equation as they contain a periodic forcing term. This is to be expected as Mathieu's equation often arises in questions of stability of motions. A two variable perturbation method on the variational equations is performed to obtain expressions for the transition curves separating regions of stability from instability. To employ the

two variable perturbation the same assumptions used in analyzing the fractional Mathieu equation were necessary. In addition to the assumptions used in analyzing the fractional Mathieu equation, an assumption on the chain rule as applied to fractional derivatives is necessary. The perturbation results are validated with numerics and, as in the fractional Mathieu problem, through direct comparison with known results in the limiting cases of fractional derivative orders $\alpha = 0$ and $\alpha = 1$.

CHAPTER 2
DIFFERENTIAL DELAY EQUATIONS

This chapter serves as an introduction to differential delay equations, DDEs. Key concepts of DDE theory are explored and illustrated by contrasting ordinary differential equations, ODEs, with DDEs. The subjects of the initial value problem and the characteristic polynomial are our main focus as they play a central role in Chapter 3.

2.1 The Initial-Value Problem

A differential delay equation relates an unknown function to its derivatives and at least one of the terms appearing in the equation has an argument that is shifted by some fixed value. If there are multiple delayed terms there may also be a corresponding number of multiple fixed shifts. Consider an example of a linear first order differential delay equation:

$$\dot{x} = -x(t - T) \tag{2.1}$$

When $T = 0$ the DDE reduces to an ODE. Note that the (2.1) is ordinary since x is only a function of one independent variable t , but since we will only be considering ordinary equations we use the term ODE to describe a non-delayed differential equation. The ODE defined by $T = 0$ requires only one point to define an initial value problem (IVP):

$$\dot{x} = -x, \quad x(t_0) = x_0 \tag{2.2}$$

Returning to the delayed equation (2.1), defining an IVP now requires an entire function rather than a discrete point as the initial condition. This “history” function, $\phi(t)$, needs to be defined on the interval $[t_0, t_0 + T]$:

$$\dot{x} = -x(t - T), \quad x(t) = \phi(t), \quad t \in [t_0, t_0 + T] \quad (2.3)$$

Equation (2.3) is of the more general type considered and categorized in [4] as a first order retarded DDE:

$$u'(t) = f(u(t), u(t - T)), \quad t > T. \quad u(t) = g(t), \quad t \in [0, T] \quad (2.4)$$

The general theorem regarding existence and uniqueness of solutions to DDEs of the form (2.4) is established and proven in [4] p.345:

Theorem 2.1: *Suppose that $g(t)$ is continuous for $0 \leq t \leq T$, with $m_g = \max_{0 \leq t \leq T} |g(t)|$, and that $f(u, v)$ satisfies a Lipschitz condition:*

$$|f(u_1, v_1) - f(u_2, v_2)| \leq c_4 (|u_1 - u_2| + |v_1 - v_2|) \quad (2.5)$$

for (u_1, v_1) and (u_2, v_2) in a region:

$$N : |u| + |v| \leq c_1.$$

Let c_2 denote the maximum of the continuous function $|f(u, v)|$ for (u, v) in N , then there exists a unique continuous solution $u(t)$ of:

$$u'(t) = f(u(t), u(t - T)), \quad t > T. \quad u(t) = g(t), \quad t \in [0, T] \quad (2.6)$$

for $0 \leq t \leq T + c_3$, where $c_3, (c_1 - 2m_g)/2c_2$.

In Theorem 2.1 t_0 is taken to be zero. This is done without the loss of generality as a variable translation may always be made to shift an initial value problem with $t_0 \neq 0$ into the form of (2.6). The existence component of Theorem 2.1 is proven in [4] by employing the method of successive approximations. In the next section the method of steps is used to solve the IVP defined by (2.3) with $T = 1$ and $\phi = 1$. This direct application of the method of steps will elucidate the continuation of ODE existence and uniqueness theory to DDEs.

2.2 Method of Steps

In the method of steps a DDE is reduced to a series of ODEs. The solution to the DDE is then found by solving over the successive intervals where the DDE has been reduced to an ODE. The existence and uniqueness of the DDE's solution can therefore be inferred based upon the application of ODE theory on each interval. The method is shown through direct application to the example IVP:

$$\dot{x} = -x(t - 1), \quad \phi(t) = 1, \quad t \in [-1, 0] \quad (2.7)$$

The initial condition function ϕ completely defines \dot{x} on the interval $[0, 1]$:

$$\dot{x} = -1, t \in [0, 1] \quad (2.8)$$

Simply integrating we obtain an expression for x on $[0, 1]$:

$$x_1 = -t + C_1, t \in [0, 1] \quad (2.9)$$

The constant C_1 is chosen so that our solution for x will be continuous, $\phi(0) = x_1(0) \Rightarrow C_1 = 1$. Continuing to the next interval:

$$\dot{x} = (t - 1) - 1, t \in [1, 2] \quad (2.10)$$

Note that the quantity $(t - 1)$ appears because x_1 is defined on $t \in [0, 1]$ but (2.10) is defined for $t \in [1, 2]$.

Integrating (2.10) and imposing $x_1(1) = x_2(1)$ for continuity we obtain:

$$x_2 = \frac{t^2}{2} - 2t + \frac{3}{2}, t \in [1, 2] \quad (2.11)$$

This process can be continued as far forward in t as desired. The iterative process is shown in Fig.2.2. The arrows depict the flow of the method, how the solution on an interval defines the derivative on the next interval, and with the derivative now defined we find the solution on that next interval. The solution obtained from the method of steps is compared and checked against the numerical results of Matlab's `dde23` routine with both solutions in agreement.

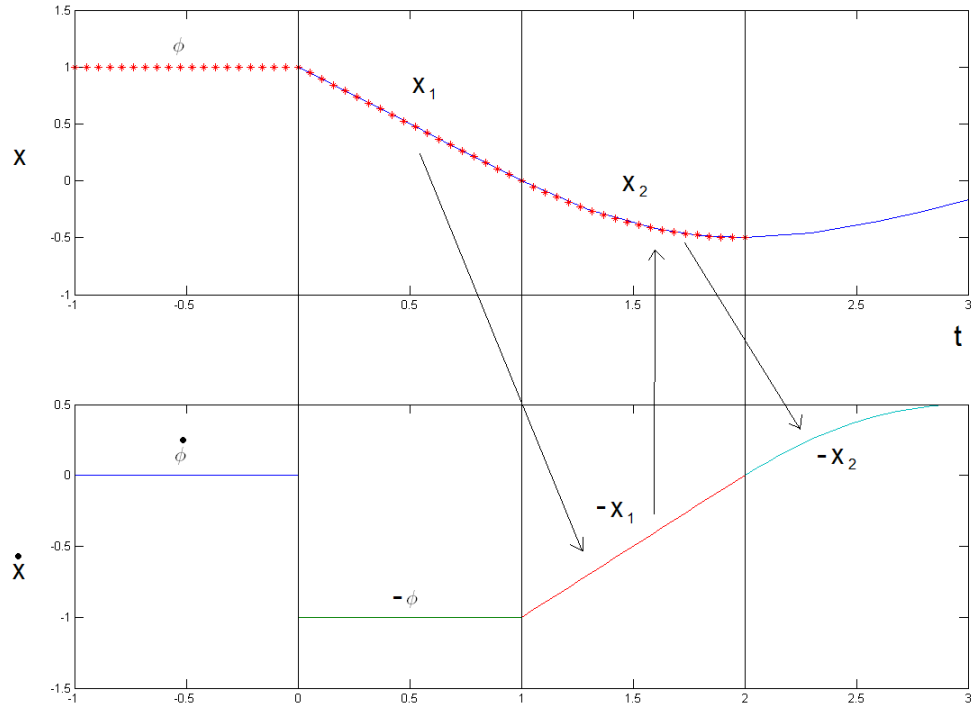


Figure 2.1: Solutions to (2.7) obtained using the method of steps (solid lines) and numerical integration using dde23 (asterisks). The arrows depict how the method of steps was performed.

2.3 The Characteristic Equation

The solution to a linear constant coefficient homogeneous ODE may be found in the form of exponentials. The same is true for DDEs. The difference however is that while the corresponding characteristic equation of an ODE is a polynomial, in the case of a DDE it will be transcendental. This transcendental nature implies an infinite number of characteristic roots and therefore an infinite family of linearly independent solutions. Returning to the example problem:

$$\dot{x} = -x(t - T) \tag{2.12}$$

Substituting the posited solution form, $x = C \exp(\lambda t)$, into (2.12) yields the transcendental characteristic equation:

$$\lambda = -\exp(\lambda T) \tag{2.13}$$

Assuming λ is complex we substitute $\lambda = a + i b$ into (2.13) and collect real and imaginary terms:

$$a = -\exp(-a T) \cos(b T) \quad b = \exp(-a T) \sin(b T) \tag{2.14}$$

As $T \rightarrow 0$ the DDE with an infinite number of characteristic roots for $T > 0$ reduces to an ODE with only one characteristic root for $T = 0$. How do we reconcile these two results? Will the solution to the DDE will converge to the solution of the ODE as $T \rightarrow 0$? Dividing the two equations of (2.13) gives an alternative expression that the characteristic roots must satisfy:

$$\frac{a}{b} = -\frac{\cos(b T)}{\sin(b T)} \tag{2.15}$$

As $T \rightarrow 0$ (2.15) becomes asymptotic to $-\frac{1}{b T}$:

$$\frac{a}{b} \sim -\frac{1}{b T}, \quad T \rightarrow 0 \tag{2.16}$$

Therefore in the limit of $T \rightarrow 0$ we see $a \rightarrow -\infty$. Since this result is independent

of b we conclude that an infinite number of roots emerge from infinity when delay is added to the system. There is one root that exists independent of the delay and corresponds to $b = 0$, $a = -1$. This root is the sole root of the corresponding $T = 0$, ODE and hence continues to exist as delay is added to the system and the additional infinite number of roots emerge from infinity.

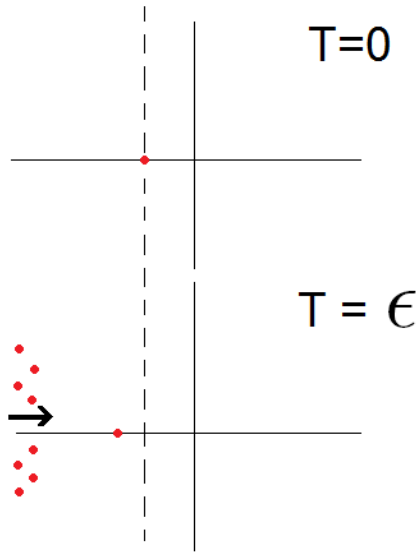


Figure 2.2: Cartoon depicting how an infinite number of characteristic roots emerge when even the smallest amount of delay is added to a system. Specifically our system (2.12) is considered which has only one root when there is no delay since it is first order.

The asymptotic behavior of the solution to a homogeneous retarded type equation, which includes (2.12), is governed by the equation's characteristic roots. Bellman and Cooke [4] provide a theorem on the asymptotic stability of an equilibrium point of a linear first order retarded DDE, p.120:

Theorem 2.2: *A necessary and sufficient condition in order that the zero solution*

of the equation:

$$a_0 u'(t) + b_0 u(t) + b_1 u(t - T) = 0 \quad (2.17)$$

be asymptotically stable in the large is that all characteristic roots have negative real part.

Bellman and Cooke go on to consider the nonlinear case:

$$a_0 u'(t) + b_0 u(t) + b_1 u(t - T) = f(u(t), u(t - T)), \quad t > T. \quad u(t) = g(t), \quad t \in [0, T] \quad (2.18)$$

and conclude that the solution will approach zero as $t \rightarrow \infty$ if the solution to the linear case, (2.17), approaches zero and if the bound m_g , as defined in Theorem 2.1, is sufficiently small, p.351 [4].

Adding the nonlinear term x^3 to (2.12) creates a nonlinear first order retarded DDE which can undergo a Hopf bifurcation.

$$\dot{x} + x^3 = -x(t - T) \quad (2.19)$$

While a Hopf bifurcation in a first order system is novel, it is identified in the usual fashion by a pair of imaginary roots in the linearized system. Recall (2.14) which gives the relations that the linear system's characteristic roots must satisfy:

$$a = -\exp(-aT) \cos(bT) \quad b = \exp(-aT) \sin(bT) \quad (2.20)$$

where the roots were assumed to be complex, $\lambda = a + ib$. Looking for pure imaginary roots we set $a = 0$:

$$0 = -\cos(bT) \quad b = \sin(bT) \quad (2.21)$$

The first expression of (2.21) implies $bT = \frac{\pi}{2} + n\pi$, where $n = 0, 1, 2, \dots$. Using this result, the second expression of (2.21) gives $b = (-1)^n$. Together these two results imply that $T = \frac{\pi}{2}$ is the smallest critical value of delay necessary for a Hopf to occur. This result is checked numerically using Matlab's dde23, Fig.2.3

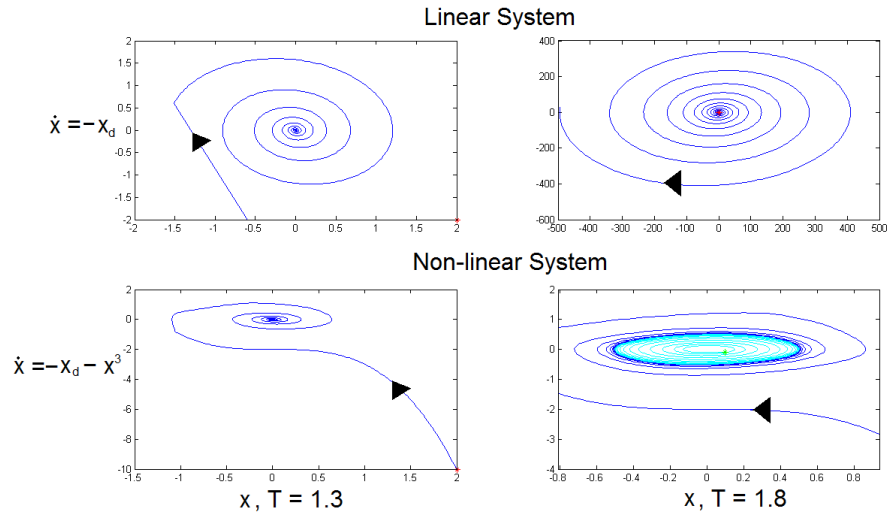


Figure 2.3: Numerical integration of linear and non-linear equations, at delays before and after the first critical Hopf value of $T = \frac{\pi}{2}$. The top row of the figure show plots of solutions to the linear equation (2.12) before and after the Hopf value and we see that the stability of the origin has changed but no limit cycle is created as the equation has no nonlinear terms. The second row of plots again shows the solution to the nonlinear equation (2.19) before and after the Hopf value where now a stable limit cycle has been born in the bifurcation.

CHAPTER 3
THE VAN DER POL OSCILLATOR UNDER DELAYED
FEEDBACK [43]

In this chapter a van der Pol type system with delayed feedback is explored. This work concerns the effect of delay on the steady state behavior of systems described by differential equations. A two variable expansion perturbation is employed and is based on choosing a critical value for the delay corresponding to a Hopf bifurcation in the unperturbed $\epsilon = 0$ system. The perturbation method will produce an amplitude-delay relation which predicts two Hopf bifurcation curves, such that in the region between these two curves oscillations will be quenched. The perturbation results are verified by comparison with numerical integration.

3.1 Introduction

The idea of a critical value of delay necessary to produce a Hopf bifurcation in a DDE was previously introduced in Section 2.3, where the simple system given by 2.19 was considered. We will now consider the following DDE:

$$\ddot{x} + x - \epsilon\gamma\dot{x} + \epsilon\alpha x^2\dot{x} = \beta\dot{x}(t - T) + \delta x(t - T) \quad (3.1)$$

This equation may be described as a version of van der Pol's equation with delay feedback. In what follows we will need to distinguish between *delay amplitude* and *delay lag*. The delay amplitudes associated with each of the terms on the right hand side of eq.(1) are β for the velocity feedback and δ for the position feedback. The delay lag is T for both terms. We will show that a change in the steady state behavior may occur in response to a change in the delay amplitudes, the delay lag,

and the other parameters of eq.(1). In particular, periodic motions may appear or disappear due to Hopf bifurcations. Knowledge of such critical parameters can be used to quench undesirable vibrations.

We begin with a review of some related literature. Considerable work has been done by other investigators on both single and coupled oscillators under delayed feedback. The literature is rich, with authors considering a wide variety of combinations of delay amplitudes and delay lags, and employing a range of perturbation techniques. The choice of which perturbation method to use is often related to the magnitude of the delay amplitude being considered. When the delay amplitude appears as $O(\epsilon)$, the method of averaging is a natural choice. Such was the approach taken in [2] - [48]. Atay [2] considered a van der Pol system under delayed position feedback, with both delay amplitude and delay lag taken as $O(\epsilon)$. The delay lag however need not be considered small in order to employ averaging, as Morrison and Rand [21] and Wirkus and Rand [48] both considered $O(1)$ delay lag in their work. Morrison and Rand [21] considered a delayed Mathieu equation, and Wirkus and Rand [48] considered two van der Pol oscillators with delay coupling. A system with delay amplitude of $O(\epsilon)$ and very large delay lag of $O(1/\epsilon)$ was investigated by Das and Chatterjee [10] using multiple time scales instead of averaging. Systems where the delay amplitude is $O(1)$ have been considered by [32] - [9]. Numerous techniques have been employed in this case with Rand and Verdugo [32] using Lindstedt's method, Maccari [17] using asymptotic perturbation, Nayfeh [24] using a center manifold reduction and finally Das and Chatterjee [9] using multiple time scales. Again, in considering $O(1)$ delay amplitude these authors have considered both $O(1)$ and $O(\epsilon)$ delay lag.

In the following sections the Hopf bifurcations of eq.(1) are explored by using the two variable expansion method. The fixed points of the resulting slow flow give an expression for the limit cycle amplitude as a function of the delay and system parameters. From the slow flow equations we determine the stability of the limit cycle created in the Hopf. We show that in a certain range of parameters, the delay lag may be chosen so as to quench the limit cycle via a Hopf bifurcation. In particular, the resulting amplitude-delay relation predicts two Hopf bifurcation curves, such that in the region between these two curves oscillations will be quenched. A similar system where both the delay amplitude and delay lag were $O(\epsilon)$ has been considered previously by Atay, [2] who used the method of averaging. In comparison with our results, the results of [2] show a single Hopf curve which corresponds to one of the two obtained by us. We compare our results with those of Atay [2] and with numerical integration.

3.2 Perturbation analysis

3.2.1 Simple harmonic oscillator with delayed feedback

Recall the van der Pol type oscillator under delayed feedback we are considering (3.1):

$$\ddot{x} + x - \epsilon\gamma\dot{x} + \epsilon\alpha x^2\dot{x} = \beta\dot{x}_d + \delta x_d \quad (3.2)$$

The subscript d denotes a delayed quantity, for example $x_d = x(t - T)$. We take the parameters ϵ , γ , α , β and δ to be positive. When $\epsilon = 0$, eq.(3.2) becomes a linear oscillator with delayed feedback:

$$\ddot{x} + x = \beta \dot{x}_d + \delta x_d \quad (3.3)$$

Observe that when $\delta \geq 1$ in eq.(3.3), we no longer have a harmonic oscillator for the case of zero delay lag. As the delay lag is increased from zero, the origin remains unstable and oscillations continue to be impossible. We therefore restrict $\delta < 1$ in what follows. We introduce the parameter T_0 , which will be the critical value of delay lag necessary for periodic solutions to eq.(3.3) to exist.

$$\ddot{x} + x = \beta \dot{x}(t - T_0) + \delta x(t - T_0) \quad (3.4)$$

Looking for periodic solutions we assume solutions of the form:

$$x = A \cos(\omega t) \quad (3.5)$$

Substituting this assumed form into (3.4) yields a set of expressions that the system parameters must satisfy:

$$\sin(\omega T_0) = -\frac{\beta \omega}{\omega^2 - 1} \quad (3.6)$$

$$\cos(\omega T_0) = -\frac{\delta}{\omega^2 - 1} \quad (3.7)$$

Squaring and adding (3.6) and (3.7) gives another form of these expressions:

$$1 = \frac{(\omega^2 - 1)^2}{\beta^2 \omega^2 + \delta^2} \Rightarrow \omega^4 - (\beta^2 + 2)\omega^2 + 1 - \delta^2 = 0 \quad (3.8)$$

Alternatively, dividing (3.6) by (3.7) yields:

$$\tan(\omega T_0) = \frac{\beta \omega}{\delta} \quad (3.9)$$

We can express ω^2 in terms of β and δ from (3.8).

$$\omega^2 = \frac{\beta^2 + 2}{2} \pm \sqrt{\left(\frac{\beta^2 + 2}{2}\right)^2 - (1 - \delta^2)} \quad (3.10)$$

which can be also be expressed as:

$$\omega^2 = \frac{\beta^2}{2} + 1 \pm \sqrt{\left(\frac{\beta^2}{2}\right)^2 + \beta^2 + \delta^2} \quad (3.11)$$

Since we consider $\delta < 1$, both roots of ω^2 will be positive and the assumed periodic solutions, eq.(3.5), will exist. This can be seen from eq.(3.10) by noting that the second term under the radical, $1 - \delta^2$, will always be positive when $\delta < 1$. This leads us to conclude the radical will always be less than the term preceding the radical. From (3.11) we observe that one root of ω will be less than 1 and the other greater than 1. This is important as the quantity $\omega^2 - 1$ will play a role in determining the stability of the limit cycle through the slow flow equations.

The vanishing denominator in eqs.(3.6),(3.7) does not represent a singularity. This may be seen by noting that from eq.(3.8), for ω to approach unity, both β and δ must approach zero. The numerator and denominator of both eqs.(3.6),(3.7) thus simultaneously vanish. To show that the limit exists, one may use L'Hospital's Rule: Substituting ω from eq.(3.10) into eqs.(3.6),(3.7) and taking the limit as β

goes to zero, where $\delta = c\beta$ for some constant c , turns out to give a nonsingular result.

In the next section we will perturb off of this solution to the $\epsilon = 0$ system in order to find approximate solutions to eq.(3.2) when $\epsilon \neq 0$.

3.2.2 Two variable expansion method

Returning to our original dde, eq.(3.2), we now perform a two variable expansion perturbation. The two variable expansion will produce slow flow equations which will capture the approach to the limit cycle, allowing us to determine its stability. Solving for the fixed points of the slow flow will give an amplitude-delay relation. For the two variable expansion we define two time scales, a slow time scale, η , and a stretched time scale, ξ . The slower time scale will capture the approach to the periodic motion.

$$\xi = \Omega t, \quad \eta = \epsilon t \tag{3.12}$$

Since we are only working to $O(\epsilon)$, without loss of generality [8], we set the time stretch to be the frequency of the $\epsilon = 0$ equation:

$$\Omega = \omega + O(\epsilon^2) \tag{3.13}$$

In terms of ξ and η our original dde , (3.2), becomes:

$$\begin{aligned} \Omega^2 \frac{\partial^2 x}{\partial \xi^2} + 2\Omega\epsilon \frac{\partial^2 x}{\partial \xi \partial \eta} + \epsilon^2 \frac{\partial^2 x}{\partial \eta^2} + x + (-\epsilon\gamma + \epsilon\alpha x^2) \left(\Omega \frac{\partial x}{\partial \xi} + \epsilon \frac{\partial x}{\partial \eta} \right) \\ = \beta \left(\Omega \frac{\partial x_d}{\partial \xi} + \epsilon \frac{\partial x_d}{\partial \eta} \right) + \delta x_d \end{aligned} \quad (3.14)$$

Next we expand x , x_d in power series:

$$x(\xi, \eta) = x_0(\xi, \eta) + \epsilon x_1(\xi, \eta) + \epsilon^2 x_2(\xi, \eta) \dots \quad (3.15)$$

$$\begin{aligned} x_d(\xi, \eta) &= x(\xi_d, \eta_d) \\ &= x_0(\xi_d, \eta_d) + \epsilon x_1(\xi_d, \eta_d) + \epsilon^2 x_2(\xi_d, \eta_d) \dots \end{aligned} \quad (3.16)$$

The delayed variables ξ_d and η_d are defined as:

$$\xi_d = \Omega(t - T) \quad (3.17)$$

$$\eta_d = \epsilon(t - T) \quad (3.18)$$

Recall that T_0 is the critical delay lag necessary for the $\epsilon = 0$ system to undergo a Hopf bifurcation. Comparing the $\epsilon \neq 0$ system with the previous $\epsilon = 0$ system, we see there is an additional linear term, $\epsilon\gamma\dot{x}$. Due to this additional linear term the critical value of delay lag necessary for a Hopf bifurcation in the $\epsilon = 0$ system will be different than T_0 . We anticipate that this additional linear term will cause only a small shift in the critical delay lag and accordingly choose to define the delay lag as:

$$T = T_0 + \epsilon\mu + O(\epsilon^2) \quad (3.19)$$

With this definition of T , (3.17) and (3.18) become:

$$\xi_d = \xi - \Omega(T_0 + \epsilon\mu + O(\epsilon^2)) \quad (3.20)$$

$$\eta_d = \eta - \epsilon(T_0 + \epsilon\mu + O(\epsilon^2)) \quad (3.21)$$

Substituting (3.13) and neglecting terms of $O(\epsilon^2)$:

$$\xi_d = \xi - \omega T_0 - \epsilon \omega \mu + \dots \quad (3.22)$$

$$\eta_d = \eta - \epsilon T_0 + \dots \quad (3.23)$$

We can now express x_d in terms of $\xi - \omega T_0$ and η by expanding it in a Taylor series about $\epsilon = 0$. We neglect terms of $O(\epsilon^2)$:

$$\begin{aligned} x_d(\xi, \eta) &= x(\xi_d, \eta_d) \\ &= \tilde{x} - \epsilon \left(\omega \mu \frac{\partial \tilde{x}}{\partial \xi} + T_0 \frac{\partial \tilde{x}}{\partial \eta} \right) \end{aligned} \quad (3.24)$$

Where in this expression we have introduced \tilde{x} for notational convenience, with \tilde{x} defined by:

$$\tilde{x} = \tilde{x}(\xi, \eta) = x(\xi - \omega T_0, \eta) \quad (3.25)$$

Substituting the power series expression for x_d , eq. (3.16), into (3.24), and again neglecting terms $O(\epsilon^2)$ we obtain a final expression for x_d .

$$x_d(\xi, \eta) = \tilde{x}_0 + \epsilon \left(\tilde{x}_1 - \omega\mu \frac{\partial \tilde{x}_0}{\partial \xi} - T_0 \frac{\partial \tilde{x}_0}{\partial \eta} \right) \quad (3.26)$$

Substituting this final expression for x_d , (3.26), and x , (3.15), into the governing equation, (3.14), and collecting terms of $O(1)$ we recover a DDE similar to eq.(3.4):

$$\omega^2 \frac{\partial^2 x_0}{\partial \xi^2} + x_0 - \delta \tilde{x}_0 - \omega\beta \frac{\partial \tilde{x}_0}{d\xi} = 0 \quad (3.27)$$

We define the left hand side of (3.27) to be $L(x_0)$.

$$L(x_0) = \omega^2 \frac{\partial^2 x_0}{\partial \xi^2} + x_0 - \delta \tilde{x}_0 - \omega\beta \frac{\partial \tilde{x}_0}{d\xi} \quad (3.28)$$

We take the general solution of (3.27) to be of the form:

$$x_0(\xi, \eta) = A(\eta) \cos(\xi) + B(\eta) \sin(\xi) \quad (3.29)$$

Substituting this general solution into the $O(1)$ DDE, (3.27), yields a set of expressions that ω and T_0 must satisfy in terms of the parameters β and δ .

$$\sin(\omega T_0) = -\frac{\beta\omega}{\omega^2 - 1} \quad (3.30)$$

$$\cos(\omega T_0) = -\frac{\delta}{\omega^2 - 1} \quad (3.31)$$

These expressions are the same as those found in the previous section, cf. eqs.(3.6),(3.7).

Again, these expressions can alternatively be expressed as eqs.(3.8),(3.9).

Returning to the step of substituting the series expansions for x , (3.15), and x_d , (3.26) into the governing equation (3.14), we now collect terms of $O(\epsilon)$.

$$\begin{aligned}
L(x_1) = & -2\omega \frac{\partial^2 x_0}{\partial \xi \partial \eta} - \omega (\alpha x_0^2 - \gamma) \frac{\partial x_0}{\partial \xi} - \omega^2 \beta \mu \frac{\partial^2 \tilde{x}_0}{\partial \xi^2} \\
& - \omega \beta T_0 \frac{\partial^2 \tilde{x}_0}{\partial \xi \partial \eta} + -\delta \omega \mu \frac{\partial \tilde{x}_0}{\partial \xi} + (\beta - \delta T_0) \frac{\partial \tilde{x}_0}{\partial \eta}
\end{aligned} \tag{3.32}$$

Next we substitute the solution form for x_0 , (3.29), into (3.32) and eliminate resonant terms by equating the coefficients of $\cos(\xi)$ and $\sin(\xi)$ to zero. Doing so yields the slow flow equations on coefficients A and B of (3.29).

$$\frac{dA}{d\eta} = \frac{G}{F} \tag{3.33}$$

$$\frac{dB}{d\eta} = \frac{H}{F} \tag{3.34}$$

$$\tag{3.35}$$

where:

$$\begin{aligned}
G = & -\omega_0 (B \beta^2 \omega_0^2 T_0 + B \delta^2 T_0 - 2 A \omega_0^3 + A \beta^2 \omega_0 + 2 A \omega_0 - B \beta \delta) \cdot \\
& (4 \omega_0^2 \gamma - 4 \gamma + 4 \beta^2 \mu \omega_0^2 - \alpha B^2 \omega_0^2 - A^2 \alpha \omega_0^2 + 4 \delta^2 \mu + \alpha B^2 + A^2 \alpha)
\end{aligned} \tag{3.36}$$

$$\begin{aligned}
H = & \omega_0 (A \beta^2 \omega_0^2 T_0 + A \delta^2 T_0 + 2 B \omega_0^3 - B \beta^2 \omega_0 - 2 B \omega_0 - A \beta \delta) \\
& (4 \omega_0^2 \gamma - 4 \gamma + 4 \beta^2 \mu \omega_0^2 - \alpha B^2 \omega_0^2 - A^2 \alpha \omega_0^2 + 4 \delta^2 \mu + \alpha B^2 + A^2 \alpha)
\end{aligned} \tag{3.37}$$

$$F = 4 \left(T_0^2 (\omega^2 - 1)^4 + (\omega^2 - 1)^2 (4\omega^2 + \beta^2 - 2\beta \delta T_0) - 4\beta^2 \omega^2 (\omega^2 - 1) \right) \tag{3.38}$$

Transforming to the general solution for x_0 , (3.29), to polar coordinates R and ψ , where $A = R \cos \psi$ and $B = R \sin \psi$, we obtain the following more tractable slow flow equations:

$$x_0(\xi, \eta) = R(\eta) \cos(\xi - \psi(\eta)) \quad (3.39)$$

$$\frac{dR}{d\eta} = \frac{D}{F} \quad (3.40)$$

$$\frac{d\psi}{d\eta} = \frac{E}{F} \quad (3.41)$$

where:

$$D = R\omega^2 (\omega^2 - 1) (2(\omega^2 - 1) - \beta^2) (4\gamma + 4\mu(\omega^2 - 1) - \alpha R^2) \quad (3.42)$$

$$E = 4T_0 \mu \omega (\omega^2 - 1)^4 + T_0 (\omega^2 - 1)^3 (4\gamma\omega - \alpha R^2) + \\ - 4\beta \delta \mu \omega (\omega^2 - 1)^2 + \beta \omega (\omega^2 - 1) (\alpha R^2 \delta - 4\delta\gamma) \quad (3.43)$$

A fixed point in the slow flow corresponds to a periodic motion in the original system. Solving for the fixed points of $\frac{dR}{d\eta}$ in (3.40) we obtain the amplitude of the periodic motion.

$$R_0^2 = \frac{4}{\alpha} \left(\gamma + \mu(\omega^2 - 1) \right) \quad (3.44)$$

Plugging this amplitude expression into $\frac{d\psi}{d\eta}$ for R^2 we find that the fixed point solutions to $\frac{dR}{d\eta}$ identically satisfy $\frac{d\psi}{d\eta}$ meaning:

$$\frac{d\psi}{d\eta} = 0 \tag{3.45}$$

Integration of (3.45) yields:

$$\psi = \psi_0 \tag{3.46}$$

This gives the final expression for the approximation to the periodic solution as:

$$x = x_0 + O(\epsilon) = R_0 \cos(\omega t - \psi_0 + O(\epsilon^2)) \tag{3.47}$$

3.2.3 Stability of the limit cycle

In addition to producing an approximation to the periodic solution, the slow flow equation on R can be used to determine the stability of the limit cycle. Recall this slow flow equation (3.40):

$$\frac{dR}{d\eta} = \frac{D}{F} \tag{3.48}$$

where D and F are given in eqs.(3.42),(3.38). We see that $\frac{dR}{d\eta}$ can be expressed in the form:

$$\frac{dR}{d\eta} = C_1 R (4C_2 - \alpha R^2) \quad (3.49)$$

where:

$$C_1 = \frac{\omega^2 (2(\omega^2 - 1) - \beta^2)}{4(T_{cr}^2 (\omega^2 - 1)^3 + (\omega^2 - 1)(4\omega^2 + \beta^2 - 2\beta\delta T_{cr}) - 4\beta^2\omega^2)} \quad (3.50)$$

$$C_2 = \gamma + \mu (\omega^2 - 1) \quad (3.51)$$

Equation (3.49) represents a slow flow on the positive R -line ($R > 0$). It has two equilibrium points, $R = 0$ and $R = \sqrt{4C_2/\alpha}$, the latter of which corresponds to the limit cycle, cf. eq.(3.44). The stability of the limit cycle will therefore be opposite to that of the origin. In order for the limit cycle to exist the quantity C_0/α must be positive. Since we are considering positive values of α , the limit cycle will therefore exist for $C_2 > 0$. The origin, $R = 0$, is unstable when the product $C_1 C_2$ is positive. In the case that the limit cycle exists C_2 satisfies $C_2 > 0$ and hence the origin will be unstable and the limit cycle stable if $C_1 > 0$. Equation (3.50) can be rewritten in the form:

$$C_1 = \frac{\omega^2 \left(2 - \frac{\beta^2}{\tilde{\omega}}\right)}{4 \left(T_{cr}^2 \beta^2 \omega^2 + 4\omega^2 \left(1 - \frac{\beta^2}{\tilde{\omega}}\right) + (\beta - \delta T_{cr})^2\right)} \quad (3.52)$$

To get C_1 in this form we used eq. (3.8) and for convenience introduced the notation $\tilde{\omega} = \omega^2 - 1$. We now ask under what parameter conditions will C_1 satisfy $C_1 > 0$, implying a stable limit cycle. Note that the denominator of (3.52) is a sum of squares except for the $\left(1 - \frac{\beta^2}{\tilde{\omega}}\right)$ term. Also note that if $\left(1 - \frac{\beta^2}{\tilde{\omega}}\right)$ is positive then

the numerator is also positive. Thus we may conclude that a sufficient condition for a stable limit cycle is:

$$\frac{\beta^2}{\tilde{\omega}} \leq 1 \tag{3.53}$$

For every possible β, δ pair (3.8) will return two values of ω . One value will be less than 1, while the other will be greater than 1. For the case of $\omega < 1$, $\tilde{\omega}$ will be negative and inequality (3.53) is satisfied. For the case of $\omega > 1$, $\tilde{\omega}$ is positive and (3.53) is no longer immediately satisfied and additional work must be done to show that (3.53) still holds. From (3.30) we can write the following inequality:

$$\frac{\beta^2 \omega^2}{\tilde{\omega}^2} \leq 1 \tag{3.54}$$

We can multiply this inequality, (3.54), by $\tilde{\omega}$ without a sign change in the inequality since we are presently considering the case of $\tilde{\omega} > 0$. Multiplying (3.54) by $\tilde{\omega}/\omega^2$ puts it in a form comparable to the inequality (3.53):

$$\frac{\beta^2}{\tilde{\omega}} \leq \frac{\tilde{\omega}}{\omega^2} \tag{3.55}$$

Expanding the right hand side of this inequality:

$$\frac{\beta^2}{\tilde{\omega}} \leq 1 - \frac{1}{\omega^2} \tag{3.56}$$

Since $\omega > 1$ we can conclude:

$$\frac{\beta^2}{\tilde{\omega}} \leq 1 - \frac{1}{\omega^2} < 1 \quad (3.57)$$

This is the inequality of (3.53) which is a sufficient condition for the limit cycle to be stable and that we set out to show was true. In summary we have shown that for both ω roots, C_1 will be positive implying that the origin is unstable and hence the limit cycle produced in the Hopf will be attracting for all values of β and δ .

3.3 Hopf bifurcation

3.3.1 Predicted Hopf bifurcation surface

A supercritical Hopf bifurcation is characterized by a stable limit cycle born with zero amplitude, growing in size. The Hopf occurs at the critical delay lag value where the limit cycle has zero amplitude. We can use the amplitude-frequency perturbation result, (3.44), to predict the critical delay lag at which a Hopf bifurcation occurs. Setting $R_0 = 0$ we obtain the critical value of μ at which the Hopf occurs.

$$\mu_{cr} = \frac{\gamma}{(1 - \omega^2)} \quad (3.58)$$

Recall that T_0 is the delay lag at which a Hopf occurs in the $\epsilon = 0$ system. However, it turns out that T_0 will not be the delay lag necessary for a Hopf in the $\epsilon > 0$ system. The critical delay lag at which the $\epsilon > 0$ system undergoes a Hopf bifurcation is given by (3.19), where μ equals μ_{cr} :

$$T_{cr} = T_0 + \epsilon \frac{\gamma}{(1 - \omega^2)} + O(\epsilon^2) \quad (3.59)$$

While this relation appears simple, in order to evaluate T_{cr} we must first solve for T_0 and ω . Recall that ω is defined by a fourth order polynomial, eq.(3.8), and is a function of β and δ , and that T_0 can only be found through an inverse trigonometric function, eqs.(3.30),(3.31) or (3.9). A closed form expression for T_{cr} in terms of β and δ is hence impossible. We can however create a T_{cr} surface plot in Matlab for the van der Pol delayed. We also look at the curves resulting from three different cuts of this surface, $\beta = 0$, $\delta = 0$ and $\beta = \delta$.

Plotting ω vs. β and δ , verifies that there are two ω roots, one less than 1 and the other greater than 1, Fig.3.1. These two roots are contained on two distinct surfaces that meet in the single point $\omega = 1$, as β and δ are decreased to zero.

Fig.3.2 shows a plot of T_{cr} vs. ω and β , and contains two surfaces, one surface for each of the two ω roots. The two T_{cr} surfaces divide the parameter space into three distinct regions. Since points on these surfaces correspond to the occurrence of Hopf bifurcations, limit cycles are generically created or destroyed as these surfaces are crossed.

In Fig.3.3 we look at three different cuts of the T_{cr} surface and confirm by numerical integration that the system transitions from oscillations to no oscillations and then back to oscillations as the delay lag is increased and the Hopf bifurcation curves are traversed. In Figs.3.4-3.6 these transitions are shown by moving from point a to b to c . Each transition is accurately predicted by the derived Hopf

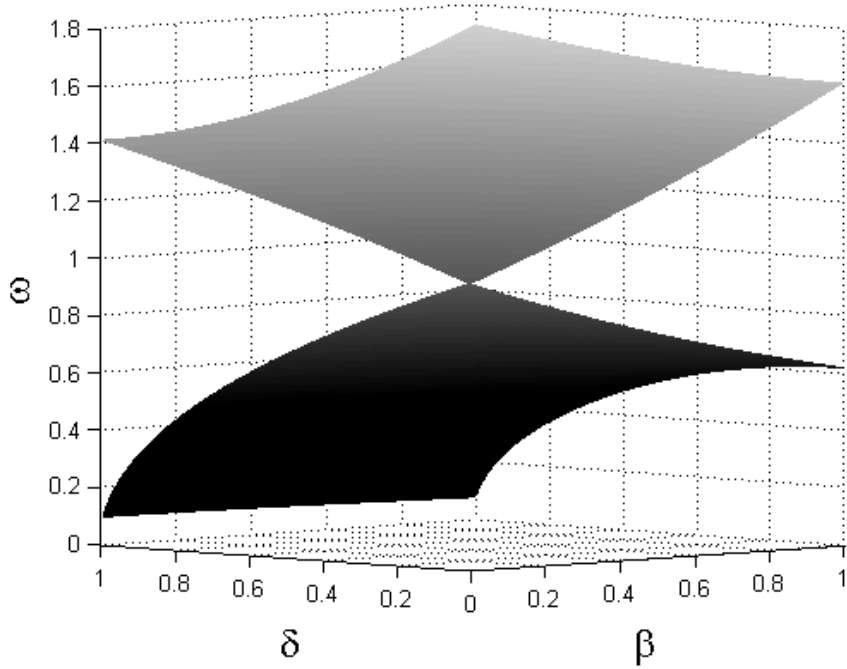


Figure 3.1: Surface plot of ω as a function of β and δ , as given by (3.8), with chosen parameters $\gamma = 1$, $\alpha = 1$.

curves. We conclude that both small ($O(\epsilon)$), and large, $O(1)$ delay lag may be used as a means to quench a limit cycle.

Additionally we can create a surface plot of T_{cr} as a function of ϵ and one of the delay amplitudes, δ or β , from equation (3.59). Recall (3.59):

$$T_{cr} = T_0 + \epsilon \frac{\gamma}{(1 - \omega^2)} + O(\epsilon^2) \quad (3.60)$$

We see that T_{cr} is linear in ϵ , with parameters T_0 and ω varying only upon β and δ . We consider and plot the case of $\beta = \delta = 0.5$, $\gamma = \alpha = 1$. The grey region in Fig.3.7 represents no oscillations, and has been found using numerical integration. We can conclude that if ϵ is increased beyond some critical value, ϵ_{cr} , the van der

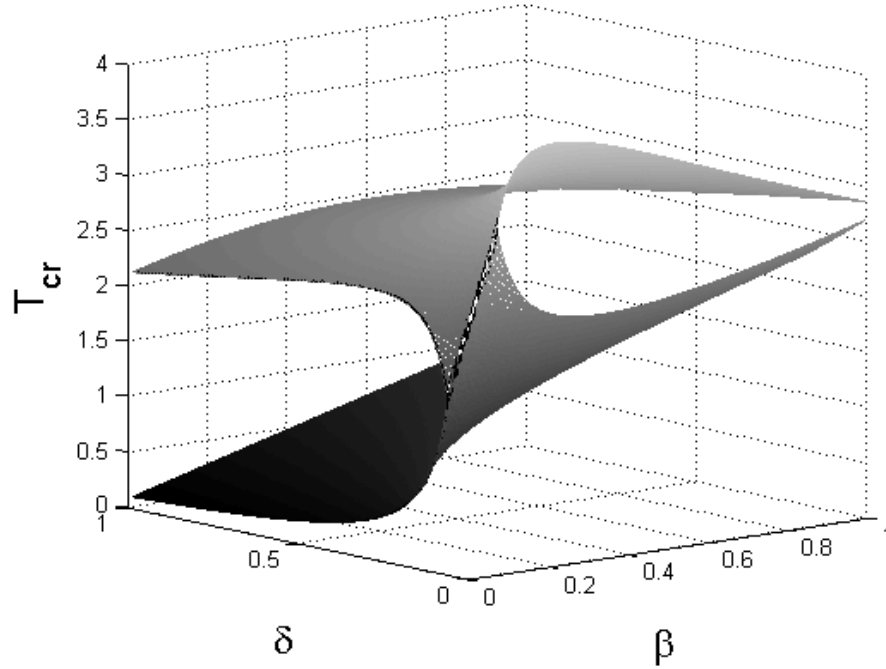


Figure 3.2: Surface plot of the critical delay lag T_{cr} necessary for a Hopf bifurcation as a function of β and δ , as given by (3.59), with chosen parameters $\gamma = 1$, $\alpha = 1$, $\epsilon = 0.1$.

Pol terms become large and the limit cycle oscillation can no longer be quenched with delay.

3.3.2 Discussion: Comparison with Atay [2]

Atay [2] considered the system:

$$\ddot{x} + x - \epsilon(1 - x^2)\dot{x} = \epsilon k x_d \quad (3.61)$$

Averaging is a natural choice for a system with $O(\epsilon)$ delay amplitude terms. Atay [2] used the method of averaging to obtain the following amplitude expression:

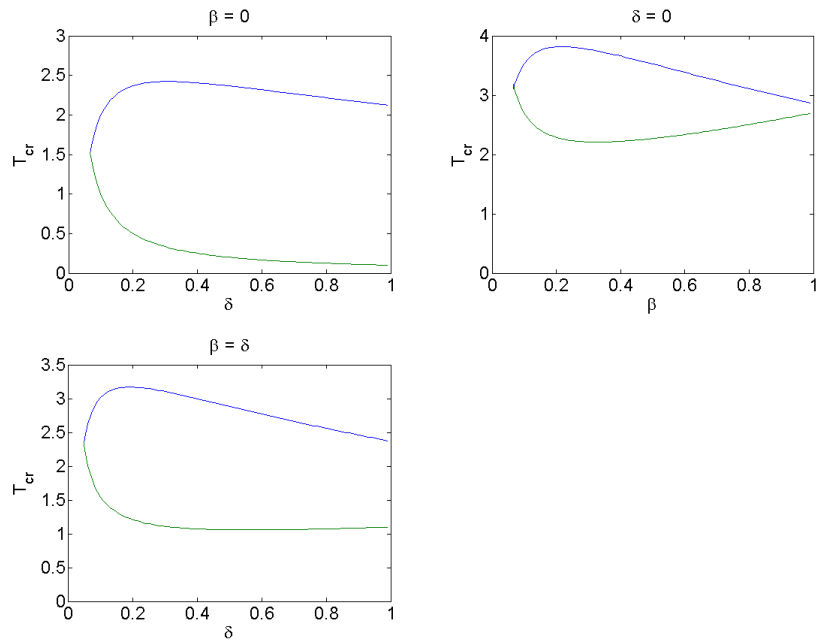


Figure 3.3: Three different cuts of the Hopf surface of Fig.3.2, defined by (3.59), where $\gamma = 1$, $\alpha = 1$, $\epsilon = 0.1$. Figure (a) shows the Hopf curve produced by cutting the Hopf surface at $\beta = 0$. Similarly (b) and (c) show the Hopf curves for $\delta = 0$ and $\beta = \delta$ respectively.

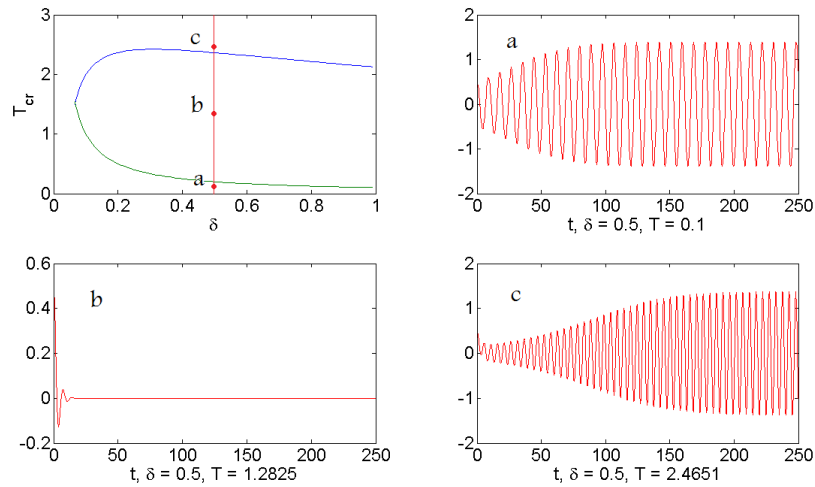


Figure 3.4: Cut at $\beta = 0$ of Hopf surface, Fig.3.2, defined by (3.59). The transition from a region of oscillation (a), to no oscillation (b), and back to oscillation (c), as the Hopf curves are crossed, for $\gamma = 1$, $\alpha = 1$, $\epsilon = 0.1$ is shown. Displayed is x versus t obtained by numerical integration of eq.(3.2).

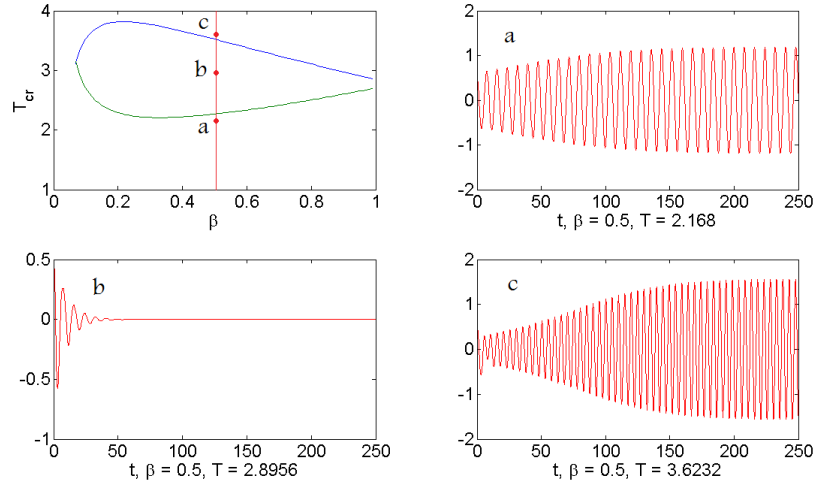


Figure 3.5: Cut at $\delta = 0$ of Hopf surface, Fig.3.2, given by (3.59). The transition from a region of oscillation (a), to no oscillation (b), and back to oscillation (c), as the Hopf curves are crossed, for $\gamma = 1$, $\alpha = 1$, $\epsilon = 0.1$ is shown. Displayed is x versus t obtained by numerical integration of eq.(3.2).

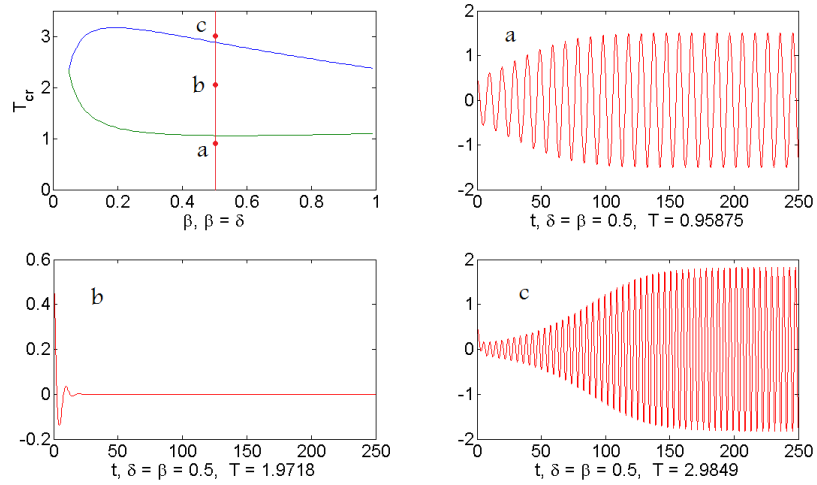


Figure 3.6: Cut at $\beta = \delta$ of Hopf surface, Fig.3.2, given by (3.59). The transition from a region of oscillation (a), to no oscillation (b), and back to oscillation (c), as the Hopf curves are crossed, for $\gamma = 1$, $\delta = 1$, $\epsilon = 0.1$ is shown. Displayed is x versus t obtained by numerical integration of eq.(3.2).

$$Amp^2 = 4(1 - k \sin(T)) \quad (3.62)$$

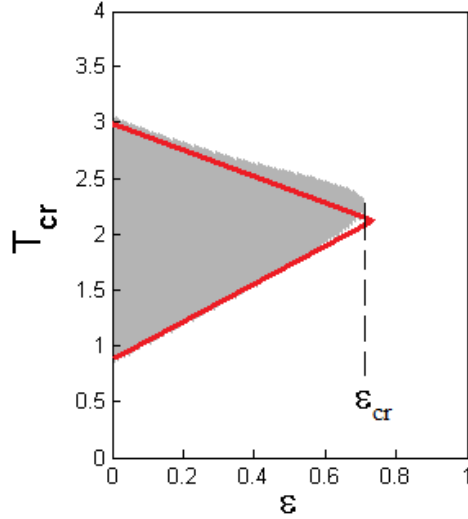


Figure 3.7: Plot of T_{cr} vs. ϵ , as given by (3.59), where $\beta = \delta = 0.5$. The grey region represents no oscillation, as concluded by numerical integration. Beyond ϵ_{cr} the oscillations may no longer be quenched with delay.

Along with an $O(\epsilon)$ delay amplitude, Atay [2] also considered the delay lag to be small ($O(\epsilon)$). Our work is instead valid for both small and large delay lag and we considered the delay amplitudes to be $O(1)$. We compare the Hopf bifurcation curve predicted by our perturbation method with the results of [2] and also numerics. We expect our curve to be in better agreement with numerics than [2] when the delay lag is large and/or the delay amplitude is large. To compare our results with [2] we again consider the case of van der Pol oscillator with delay, setting γ and α equal to one in our system (3.2). Additionally we need to equate our delay amplitudes with those of [2] implying, $\delta = \epsilon k$ and $\beta = 0$. The Hopf curves are plotted over $0 < k < 1/\epsilon$. This range was chosen, recalling that $\delta < 1$ is necessary for oscillation.

In Fig.3.8 it is seen our results for small delay lag agree with Atay's. For large delay lag however the results diverge. This divergence grows when the delay lag

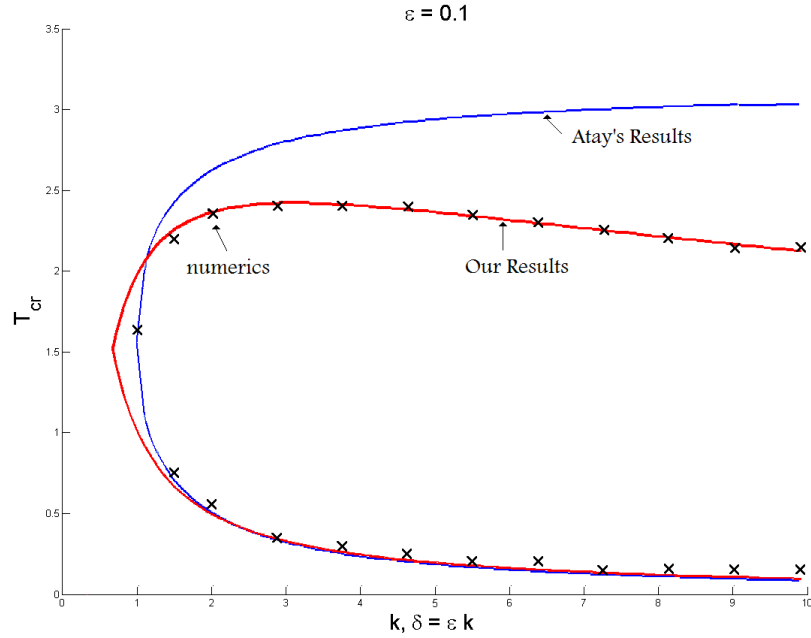


Figure 3.8: Comparison of our Hopf bifurcation curve, eq.(3.44), vs. Atay's [2], eq.(3.62), which is based on assuming both small delay amplitude and small delay lag. x 's represent numerical integration of eq.(3.2). Parameters taken as, $\gamma = 1$, $\alpha = 1$, $\beta = 0$, $\epsilon = 0.1$.

is large and the delay amplitude k is increased to also become large. As expected when T_{cr} is large or when k is large our results are in better agreement with numerics than the results in [2].

3.4 Summary

In this chapter a van der Pol type system under delayed feedback, (3.1), with delay amplitudes of $O(1)$ and delay lags not necessarily small was considered. The two variable expansion perturbation scheme we used is based on choosing a critical value for the delay corresponding to a Hopf bifurcation in the unperturbed $\epsilon = 0$

system. The perturbation method yielded two Hopf bifurcation curves, which were verified numerically. These two Hopf curves bound a region of no oscillation, see Figs. 3.4-3.6. Oscillations may be quenched by appropriately varying the delay lag, so as to enter this region. We have therefore shown that delay may be used as a means to control and quench undesirable limit cycle oscillations.

CHAPTER 4
THE FRACTIONAL CALCULUS

The fractional calculus and fractional differential equations have recently become increasingly important topics in the literature of engineering, science and applied mathematics. Application areas include viscoelasticity, electromagnetics, heat conduction, control theory and diffusion [28],[18],[15],[12],[14],[19]. One reason for the interest in this subject comes from applications which involve new ways of modeling physical systems using tools from fractional calculus. For example, consider the dynamics of a system which involves the motion of a rheological specimen which exhibits both elasticity and dissipation. Traditional models of such a system might be based on the following familiar linear differential equation:

$$x'' + cx' + kx = 0 \tag{4.1}$$

However, an alternative approach would be to combine the effects of stiffness and damping in a single term:

$$x'' + \mu D^\alpha x = 0 \tag{4.2}$$

where $D^\alpha x$ is the order α derivative of $x(t)$, where $0 < \alpha < 1$ is a parameter, and where μ is a coefficient of “fractance”. As α varies from 0 to 1, the relative importance of the stiffness and damping terms may be adjusted. See e.g. [46]. Note that eq.(4.2) is linear.

As this simple example illustrates, the fractional derivative operator is an extension of the familiar integer order derivative to arbitrary order including integer, rational, irrational and complex values. In section 4.1 an integral expression is derived to represent the fractional derivative. Viewing the fractional derivative in this context

of integration it is clear that the fractional derivative will depend on the upper and lower limits, with different choices of these limits leading to different definitions. For this reason authors often use the notation ${}_c D_t^\alpha x(t)$, where c is the lower limit. When $c = 0$ the integral representation is attributed to Riemann and Liouville and called the Riemann-Liouville integral. The Riemann-Liouville integral is a commonly chosen representation for the fractional derivative in research papers and is the definition we employ in our work. Since we will be using only the Riemann-Liouville integral representation we adopt the abbreviated notation:

$$D^\alpha x(t) \equiv {}_0 D_t^\alpha x(t) \quad (4.3)$$

There are various methods for obtaining the Riemann-Liouville integral, with Ross [36] outlining four distinct approaches. We offer a formal derivation section 4.1 beginning with an intuitive definition of the fractional derivative of t^k , $D^\alpha t^k$. By “formal” we mean that issues of convergence will be ignored. This formal derivation may thus be thought of as a plausibility argument rather than a rigorous derivation. A key step in our derivation is the use of an identity attributed to Euler:

$$\int_0^t (t-u)^m u^n du = \frac{m! n!}{(m+n+1)!} t^{m+n+1} = \frac{\Gamma(m+1)\Gamma(n+1)}{\Gamma(m+n+2)} t^{m+n+1} \quad (4.4)$$

The use of this identity is one of the four approaches outlined by Ross [36]. Additionally see e.g. [25],[28],[20],[39],[16].

The chapter is closed with section 4.2 in which three methods for solving fractional differential equations are considered. We seek solutions using the Laplace transform method, by positing a power series solution and finally by numerical

integration. These methods are shown through example with each method being applied to the simple linear fractional differential equation previously posed in (4.2:

$$x'' + \mu D^\alpha x = 0 \tag{4.5}$$

with $0 < \alpha < 1$.

4.1 Fractional Derivatives

We begin with a intuitive definition for the fractional derivative of t^k , $D^\alpha t^k$. From there we derive an integral expression for the fractional derivative. Issues of convergence are ignored in our derivation and it may therefore be thought of as a plausibility argument instead of a rigorous derivation. After Ross [36], we note that:

$$\frac{d^m}{dt^m} t^n = \frac{n!}{(n-m)!} t^{n-m} \tag{4.6}$$

where $m \leq n$ are positive integers. Note that eq.(4.6) can be written in terms of the gamma function $\Gamma(n+1) = n!$:

$$\frac{d^m}{dt^m} t^n = \frac{\Gamma(n+1)}{\Gamma(n-m+1)} t^{n-m} \tag{4.7}$$

By using the gamma function we can now generalize (4.7) to include all positive real numbers by replacing n by k and m by α , where k and α are positive real numbers, we obtain:

$$D^\alpha t^k = \frac{\Gamma(k+1)}{\Gamma(k-\alpha+1)} t^{k-\alpha} \quad (4.8)$$

As an example, we compute the order 1/2 derivative of t :

$$D^{1/2} t = \frac{\Gamma(2)}{\Gamma(3/2)} t^{1/2} = \frac{2}{\sqrt{\pi}} t^{1/2} \quad (4.9)$$

By the law of exponents of derivatives:

$$D^{1/2} D^{1/2} t = D^{1/2+1/2} t = \frac{d}{dt} t = 1 \quad (4.10)$$

Using this result from the law of exponents we check (4.9) by taking the order 1/2 derivative of it:

$$D^{1/2} \frac{2}{\sqrt{\pi}} t^{1/2} = \frac{2}{\sqrt{\pi}} D^{1/2} t^{1/2} = \frac{2}{\sqrt{\pi}} \frac{\Gamma(3/2)}{\Gamma(1)} t^0 = 1 \quad (4.11)$$

Now suppose we have a function $x(t)$ which is expandable in a Taylor series about $t = 0$:

$$x(t) = \sum \frac{x^{(k)}(0)}{k!} t^k \quad (4.12)$$

where $x^{(k)}(0)$ is the k^{th} derivative of x evaluated at $t = 0$. Taking the fractional derivative of both sides:

$$D^\alpha x(t) = \sum \frac{x^{(k)}(0)}{k!} D^\alpha t^k = \sum \frac{x^{(k)}(0)}{k!} \frac{\Gamma(k+1)}{\Gamma(k-\alpha+1)} t^{k-\alpha} \quad (4.13)$$

After Ross [36] we note that:

$$\int_0^t (t-u)^m u^n du = \frac{m! n!}{(m+n+1)!} t^{m+n+1} = \frac{\Gamma(m+1)\Gamma(n+1)}{\Gamma(m+n+2)} t^{m+n+1} \quad (4.14)$$

We look to use (4.14) in simplifying (4.13) and hence $t^{k-\alpha} = t^{m+n+1}$. This yields an appropriate change of variables $n = k$ and $m = -1 - \alpha$ and (4.14) becomes:

$$\int_0^t (t-u)^{-1-\alpha} u^k du = \frac{\Gamma(-\alpha) \Gamma(k+1)}{\Gamma(k-\alpha+1)} t^{k-\alpha} \quad (4.15)$$

Solving for the common term appearing in (4.13):

$$\frac{\Gamma(k+1)}{\Gamma(k-\alpha+1)} t^{k-\alpha} = \frac{1}{\Gamma(-\alpha)} \int_0^t (t-u)^{-1-\alpha} u^k du \quad (4.16)$$

Substituting (4.16) into (4.13) we obtain:

$$D^\alpha x(t) = \sum \frac{x^{(k)}(0)}{k!} \frac{1}{\Gamma(-\alpha)} \int_0^t (t-u)^{-1-\alpha} u^k du \quad (4.17)$$

Interchanging the processes of summation and integration, we obtain:

$$D^\alpha x(t) = \frac{1}{\Gamma(-\alpha)} \int_0^t (t-u)^{-1-\alpha} \left\{ \sum \frac{x^{(k)}(0) u^k}{k!} \right\} du \quad (4.18)$$

Recognizing our original Taylor expansion for $x(t)$, (4.12), we obtain:

$$D^\alpha x(t) = \frac{1}{\Gamma(-\alpha)} \int_0^t (t-u)^{-1-\alpha} x(u) du \quad (4.19)$$

If α is negative then (4.19) defines the fractional integral. We however are interested in defining the fractional derivative and $\alpha > 0$. To avoid divergence of the Gamma function in eq.(4.19), we use a trick from Ross [36]. From the law of exponents of derivatives we write:

$$D^\alpha x(t) = D^m D^{-p} x(t) \quad (4.20)$$

where $\alpha = m - p$, where $0 < p < 1$ and where m is the least integer larger than α . Using eq.(4.19), we obtain:

$$D^\alpha x(t) = \frac{d^m}{dt^m} \frac{1}{\Gamma(p)} \int_0^t (t-u)^{p-1} x(u) du \quad (4.21)$$

For the case of $0 < \alpha < 1$, we have that $m = 1$ and $p = 1 - \alpha$, giving:

$$D^\alpha x(t) = \frac{1}{\Gamma(1-\alpha)} \frac{d}{dt} \int_0^t (t-u)^{-\alpha} x(u) du \quad (4.22)$$

For example:

$$D^{1/2} x(t) = \frac{1}{\Gamma(1/2)} \frac{d}{dt} \int_0^t (t-u)^{-1/2} x(u) du \quad (4.23)$$

As a check we use this formula to compute the order 1/2 derivative of t :

$$D^{1/2} t = \frac{1}{\Gamma(1/2)} \frac{d}{dt} \int_0^t (t-u)^{-1/2} u du = \frac{1}{\Gamma(1/2)} \frac{d}{dt} \left(\frac{4}{3} t^{3/2} \right) = \frac{2}{\sqrt{\pi}} t^{1/2} \quad (4.24)$$

which agrees with eq.(4.9). Eq.(4.22) can be simplified by taking $v = t - u$, giving:

$$D^\alpha x(t) = \frac{1}{\Gamma(1-\alpha)} \frac{d}{dt} \int_0^t v^{-\alpha} x(t-v) dv \quad (4.25)$$

Carrying out the differentiation under the integral sign, we obtain:

$$D^\alpha x(t) = \frac{1}{\Gamma(1-\alpha)} \left(\int_0^t v^{-\alpha} x'(t-v) dv + \frac{x(0)}{t^\alpha} \right) \quad (4.26)$$

After Ross [36], p.17, we adopt the convention that $x(0) = 0$, giving the final formula:

$$D^\alpha x(t) = \frac{1}{\Gamma(1-\alpha)} \int_0^t v^{-\alpha} x'(t-v) dv \quad (4.27)$$

4.2 Several Methods for Solving Fractional Differential Equations

In this section we consider three methods for solving fractional differential equations the Laplace transform method, the power series method and numerical integration. The methods are discussed and outlined through direct application to the simple linear fractional differential:

$$x'' + \mu D^\alpha x = 0 \quad (4.28)$$

with $0 < \alpha < 1$.

This is the same equation that was discussed briefly in the beginning of the chapter,

(4.2). Recall that this equation can be viewed as a way of modeling a damped mass spring system:

$$x'' + cx' + kx = 0 \tag{4.29}$$

where now the stiffness, x , and damping, x' , terms are now both encompassed in the single fractional derivative term. As α varies from 0 to 1, the relative importance of the stiffness and damping terms are adjusted. See e.g. [46]. We therefore expect the system to behave like a damped oscillator for all values $0 < \alpha < 1$ with the response decaying to zero as time $t \rightarrow \infty$. This is the result we recover in all three methods. Additionally all three methods agree in the transient response.

4.2.1 Laplace transform approach

The Laplace transform method is a familiar and convenient approach for solving linear ordinary differential equations with initial conditions. In this section we show through example how the Laplace transform method may also be used to solve linear fractional differential equations. The Laplace transform L is an integral operator which when applied to a function $x(t)$ yields a new function $X(s)$ with new independent variable s . Applying the Laplace transform to a differential equation converts it into an algebraic equation which may be easier to solve. The Laplace transform of a function $x(t)$ that is defined for all $t \geq 0$ is given by:

$$X(s) = L\{x(t)\} = \int_0^{\infty} e^{-st}x(t)dt \tag{4.30}$$

Consider the second order linear fractional differential equation:

$$x'' + \mu D^\alpha x = 0 \quad (4.31)$$

where $0 < \alpha < 1$. Applying the Laplace transform to (4.31) yields:

$$L\{x''(t)\} + \mu L\{D^\alpha x(t)\} = 0 \quad (4.32)$$

The Laplace transform of x'' exists for $s > c$ when x is continuous, piecewise smooth and $|x|$ is bounded by $M e^{ct}$ as $t \rightarrow \infty$. If these conditions hold, applying (4.30) and using integration by parts twice gives:

$$L\{x''(t)\} = \int_0^\infty e^{-st} x''(t) dt \quad (4.33)$$

$$= x'(t) e^{-st} \Big|_0^\infty + \int_0^\infty e^{-st} x'(t) dt \quad (4.34)$$

$$= x'(t) e^{-st} \Big|_0^\infty + s x(t) e^{-st} \Big|_0^\infty + \int_0^\infty e^{-st} x(t) dt \quad (4.35)$$

$$= s^2 X(s) - s x(0) - x'(0) \quad (4.36)$$

Returning to our transformed fractional differential equation (4.32) what remains to be defined is the Laplace transform of $D^\alpha x$. In the derivation of $L\{D^\alpha x(t)\}$ we make use of the convolution property of the Laplace transform. As in section 4.1 our derivation is not rigorous and issues of convergence will be ignored. For a complete analysis and treatment of $0 \not\leq \alpha \not\leq 1$ the reader is again referred to [36]. The convolution $f * g$ of the piecewise functions f and g is defined for $t \geq 0$ as:

$$(f * g)(t) = \int_0^t f(\tau) g(t - \tau) d\tau \quad (4.37)$$

Using a change of variable $u = t - \tau$ one can see that the convolution is commutative, $f * g = g * f$. If in addition to being piecewise continuous $|f(t)|$ and $|g(t)|$ are bounded by $M e^{ct}$ as $t \rightarrow \infty$ then the Laplace transform of $f * g$ exists for $s > c$ and is given by:

$$L\{(f * g)(t)\} = L\{f(t)\} L\{g(t)\} \quad (4.38)$$

Recall eq.(4.22) which uses the law of exponents of derivatives to write $D^\alpha x(t)$, $0 < \alpha < 1$, as:

$$D^\alpha x(t) = \frac{1}{\Gamma(1 - \alpha)} \frac{d}{dt} \int_0^t (t - u)^{-\alpha} x(u) du \quad (4.39)$$

Using the fact that $L\{D h(t)\} = s L\{h(t)\} - h(0)$ and viewing the integral part of (4.39) as h the Laplace transform of (4.39) is:

$$L\{D^\alpha x(t)\} = \frac{1}{\Gamma(1 - \alpha)} \left[s L \left\{ \int_0^t (t - u)^{-\alpha} x(u) du \right\} - \left[\int_0^t (t - u)^{-\alpha} x(u) du \right] \Big|_{t=0} \right] \quad (4.40)$$

$$= \frac{s}{\Gamma(1 - \alpha)} L \left\{ \int_0^t (t - u)^{-\alpha} x(u) du \right\} \quad (4.41)$$

Observe that (4.41) is of the form of a convolution integral. Applying the convolution property of the Laplace transform to (4.41) gives:

$$L\{D^\alpha x(t)\} = \frac{s}{\Gamma(1 - \alpha)} L\{t^{-\alpha}\} L\{x(t)\} \quad (4.42)$$

Using the identity $L\{t^\mu\} = \frac{\Gamma(\mu+1)}{s^{\mu+1}}$, ($\mu > -1$), yields the final expression:

$$L\{D^\alpha x(t)\} = s^\alpha X(s) \quad (4.43)$$

Substituting our definitions for $L\{x''(t)\}$, (4.36), and $L\{D^\alpha x(t)\}$, (4.43), into (4.32) our fractional differential equation is transformed into the algebraic equation:

$$(s^2 + \mu s^\alpha) X - s x(0) - x'(0) = 0 \quad (4.44)$$

At this point we simplify the problem by setting $\mu = 1$, $x(0) = 0$, and $x'(0) = 1$:

$$(s^2 + s^\alpha) X - 1 = 0 \quad (4.45)$$

Solving for X :

$$X = \frac{1}{s^2 + s^\alpha} \quad (4.46)$$

Having solved for X , the problem now becomes taking the inverse Laplace transform of (4.46). If α were not fractional and instead an integer, we would proceed by decomposing the right hand side into partial fractions and then find the inverse Laplace transform of each partial fraction. Since we are considering a fractional α we insert an intermediate step. This step is to introduce a new variable y , where $y = s^{1/v}$. The v is chosen as the lowest common denominator of the exponents of s . By defining y in this fashion each of the terms appearing in the polynomial can be written in the form of y^n where n is an integer and the method of partial fractions may be applied in its usual form. To proceed we again simplify the problem setting

$\alpha = 1/2$. This choice of α implies $v = 2$ and $y = s^{1/2}$. The right hand side of (4.46) becomes:

$$\frac{1}{y^4 + y} \tag{4.47}$$

It is decomposed into the sum of four partial fractions:

$$\frac{1}{y^4 + y} = \frac{1}{y} - \frac{1}{3} \left(\frac{1}{y+1} \right) - \frac{1}{3} \left(\frac{1}{y-r} \right) - \frac{1}{3} \left(\frac{1}{y-\bar{r}} \right) \tag{4.48}$$

where, $r = \exp(-i\pi/3)$ and its complex conjugate $\bar{r} = \exp(i\pi/3)$. Transforming back to s :

$$\frac{1}{s^2 + s^{1/2}} = \frac{1}{s^{1/2}} - \frac{1}{3} \left(\frac{1}{s^{1/2} + 1} \right) - \frac{1}{3} \left(\frac{1}{s^{1/2} - r} \right) - \frac{1}{3} \left(\frac{1}{s^{1/2} - \bar{r}} \right) \tag{4.49}$$

Each of the terms in (4.49) are of the form $s^{1/2} - \sigma$. Note that these terms may be factored and alternatively expressed as:

$$\frac{1}{s^{1/2} - \sigma} = \frac{1}{s^{-1/2} (s - \sigma^2)} + \frac{\sigma}{s - \sigma^2} \tag{4.50}$$

The function E_t is a function frequently arising in fractional calculus. We are following the notation of [36] in calling it E_t . The function is defined as being the fractional integral of an exponential.

$$D^{-\alpha} e^{at} = E_t(\alpha, a), \quad \alpha > 0 \tag{4.51}$$

Applying the definition for fractional integration (4.19) gives the integral expression for E_t :

$$D^{-\alpha} e^{at} = \frac{1}{\Gamma(\alpha)} \int_0^t (t-v)^{\alpha-1} e^{av} dv, \quad \alpha > 0 \quad (4.52)$$

$$= E_t(\alpha, a) \quad (4.53)$$

The Laplace transform of E_t is easily computed by utilizing the convolution theorem cf. (4.37)-(4.38).

$$L \{E_t(\alpha, a)\} = L \left\{ \frac{1}{\Gamma(\alpha)} \int_0^t (t-v)^{\alpha-1} e^{av} dv \right\}, \quad \alpha > 0 \quad (4.54)$$

$$= \frac{1}{\Gamma(\alpha)} L \{t^{\alpha-1}\} L \{e^{at}\} \quad (4.55)$$

$$= \left(\frac{1}{\Gamma(\alpha)} \right) \left(\frac{\Gamma(\alpha)}{s^\alpha} \right) \left(\frac{1}{s-a} \right) \quad (4.56)$$

$$= \frac{1}{s^\alpha(s-a)} \quad (4.57)$$

Using the result of (4.57) we observe the useful inverse Laplace relation:

$$L^{-1} \left\{ \frac{1}{s^\nu (s-\sigma^2)} \right\} = E_t(\nu, \sigma^2) \quad (4.58)$$

Recall the common form of the partial fraction factors, cf. (4.50):

$$\frac{1}{s^{1/2} - \sigma} = \frac{1}{s^{1/2} (s - \sigma^2)} + \frac{\sigma}{s - \sigma^2} \quad (4.59)$$

Combining (4.58) and (4.59) we find:

$$L^{-1} \left\{ \frac{1}{s^{1/2} - \sigma} \right\} = E_t(-1/2, \sigma^2) + \sigma E_t(0, \sigma^2) \quad (4.60)$$

Returning to our instructional example we require the inverse Laplace transform of (4.46) where $\alpha = 1/2$. Equation (4.46) is decomposed using (4.49) and applying (4.60) yields:

$$\begin{aligned} x(s) = & E_t(-1/2, 0) - \frac{1}{3} [E_t(-1/2, 1) - E_t(0, 1)] - \frac{1}{3} [E_t(-1/2, r^2) + r E_t(0, r^2)] \\ & - \frac{1}{3} [E_t(-1/2, \bar{r}^2) + \bar{r} E_t(0, \bar{r}^2)] \end{aligned} \quad (4.61)$$

The function E_t has takes special forms for select values of α and a :

$$E_t(0, a) = e^{at} \quad (4.62)$$

$$E_t(1/2, a) = a^{-1/2} e^{at} \operatorname{Erf}(at)^{1/2} \quad (4.63)$$

$$E_t(-1/2, a) = a E_t(1/2, a) + \frac{1}{\sqrt{\pi t}} \quad (4.64)$$

$$= a^{1/2} e^{at} \operatorname{Erf}(at)^{1/2} + \frac{1}{\sqrt{\pi t}} \quad (4.65)$$

$$E_t(\nu, 0) = \frac{t^\nu}{\Gamma(\nu + 1)} \quad (4.66)$$

Using these identities (4.61) becomes:

$$\begin{aligned} x(t) = & \frac{1}{\sqrt{\pi t}} - \frac{1}{3} \left[e^t \operatorname{Erf}\sqrt{t} + \frac{1}{\sqrt{\pi t}} - e^t \right] - \frac{1}{3} \left[r e^{r^2 t} \operatorname{Erf}(r\sqrt{t}) + \frac{1}{\sqrt{\pi t}} + r e^{r^2 t} \right] \\ & - \frac{1}{3} \left[\bar{r} e^{\bar{r}^2 t} \operatorname{Erf}(\bar{r}\sqrt{t}) + \frac{1}{\sqrt{\pi t}} + \bar{r} e^{\bar{r}^2 t} \right] \end{aligned} \quad (4.67)$$

Simplifying:

$$x(t) = -\frac{1}{3} \left[e^t \operatorname{Erf} \sqrt{t} - e^t \right] - \frac{1}{3} \left[r e^{r^2 t} \operatorname{Erf}(r\sqrt{t}) + r e^{r^2 t} \right] - \frac{1}{3} \left[\bar{r} e^{\bar{r}^2 t} \operatorname{Erf}(\bar{r}\sqrt{t}) + \bar{r} e^{\bar{r}^2 t} \right] \quad (4.68)$$

Substituting the definition of the Error function:

$$x(t) = -\frac{1}{3} \left[\frac{2e^t}{\sqrt{\pi}} \int_0^{\sqrt{t}} e^{-z^2} dz - e^t \right] - \frac{1}{3} \left[\frac{2r e^{r^2 t}}{\sqrt{\pi}} \int_0^{r\sqrt{t}} e^{-z^2} dz + r e^{r^2 t} \right] - \frac{1}{3} \left[\frac{2\bar{r} e^{\bar{r}^2 t}}{\sqrt{\pi}} \int_0^{\bar{r}\sqrt{t}} e^{-z^2} dz + \bar{r} e^{\bar{r}^2 t} \right] \quad (4.69)$$

To plot this solution (4.68) in Matlab we replace the Error function with its Taylor series expansion:

$$\operatorname{Erf}(t) = \frac{2}{\sqrt{\pi}} \int_0^t e^{-z^2} dz \quad (4.70)$$

$$= \frac{2}{\sqrt{\pi}} \int_0^t \sum_{n=0}^{\infty} \frac{(-1)^n z^{2n}}{n!} dz \quad (4.71)$$

$$= \frac{2}{\sqrt{\pi}} \sum_{n=0}^{\infty} \frac{(-1)^n t^{2n+1}}{(2n+1)n!} \quad (4.72)$$

The short Matlab script used to plot the solution (4.68) is given in appendix A.1 with the Taylor series (4.72) truncated at 200 terms. The solution obtain by the Laplace method is shown in Fig.4.1.

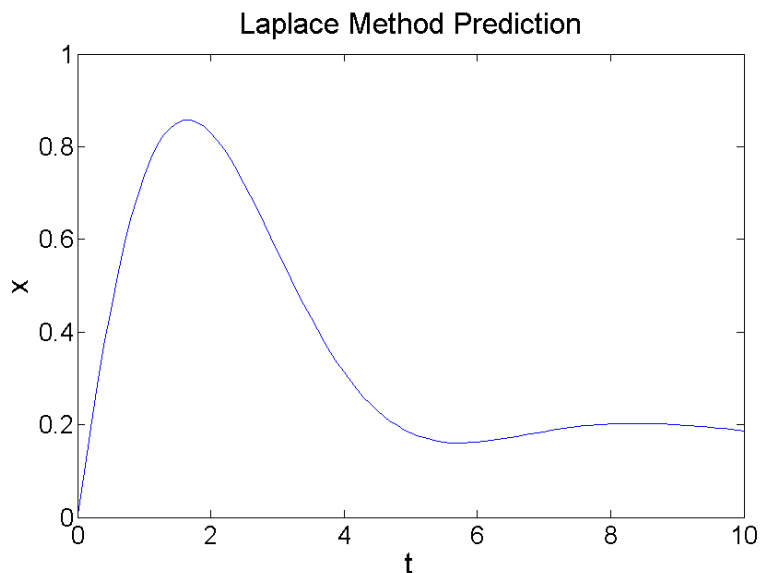


Figure 4.1: Solution to (4.31) with $\mu = 1$ and $\alpha = 1/2$ given by (4.68) with (4.72) found using the Laplace transform method.

4.2.2 Power Series Approach

Another method used to solve integer order differential equations that may also be applied to fractional differential equations is the power series method. It is possible to extend this method to fractional differential equations since the derivative of a power series is also a power series. Recall the system we are considering:

$$x'' + \mu D^\alpha x = 0 \tag{4.31}$$

where $0 < \alpha < 1$.

We begin the method by assuming a solution of the form:

$$x(t) = \sum_{n=0}^{\infty} C_n t^{\frac{n}{\nu}} \tag{4.73}$$

The second derivative of $x(t)$, $x''(t)$, is given by:

$$x''(t) = \sum_{n=1}^{\infty} \frac{n}{v} \left(\frac{n}{v} - 1 \right) C_n t^{\frac{n}{v}-2} \quad (4.74)$$

Recalling (4.8) $D^\alpha x(t)$ takes the form:

$$D^\alpha x(t) = \sum_{n=0}^{\infty} \frac{\Gamma\left(\frac{n}{v} + 1\right)}{\Gamma\left(\frac{n}{v} + 1 - \alpha\right)} C_n t^{\frac{n}{v}-\alpha} \quad (4.75)$$

Substituting (4.74) and (4.75) into (4.31):

$$\sum_{n=1}^{\infty} \frac{n}{v} \left(\frac{n}{v} - 1 \right) C_n t^{\frac{n}{v}-2} + \mu \sum_{n=0}^{\infty} \frac{\Gamma\left(\frac{n}{v} + 1\right)}{\Gamma\left(\frac{n}{v} + 1 - \alpha\right)} C_n t^{\frac{n}{v}-\alpha} = 0 \quad (4.76)$$

In order for the fractional derivative, $D^\alpha x(t)$, to balance with $x''(t)$ observe that v must be equal to the denominator of α . For a system containing multiple fractional derivatives an appropriate choice for v is the lowest common denominator of the appearing fractional orders. We again consider the case of $\alpha = 1/2$ implying then that $v = 2$. Setting $\alpha = 1/2$, $\mu = 1$ and $v = 2$ in (4.76):

$$\sum_{n=1}^{\infty} \frac{n(n-2)}{4} C_n t^{\frac{n-4}{2}} + \sum_{n=0}^{\infty} \frac{\Gamma\left(\frac{n+4}{2}\right)}{\Gamma\left(\frac{n+3}{2}\right)} C_n t^{\frac{n-1}{2}} = 0 \quad (4.77)$$

Re-indexing:

$$-\frac{1}{4} C_1 t^{-3/2} + \sum_{n=0}^{\infty} \left(\frac{(n+3)(n+1)}{4} C_{n+3} + \frac{\Gamma\left(\frac{n+4}{2}\right)}{\Gamma\left(\frac{n+3}{2}\right)} C_n \right) t^{\frac{n-1}{2}} = 0 \quad (4.78)$$

The initial conditions are again chosen as $x(0) = 0$ and $x'(0) = 1$ which imply

$C_0 = 0$ and $C_1 = 0$, $C_2 = 1$ respectively. From (4.78) the recursive relation for the C_n coefficients is given by:

$$C_n = -\frac{4\Gamma\left(\frac{n+4}{2}\right)}{\Gamma\left(\frac{n+3}{2}\right)(n+3)(n+1)}C_{n-3}, \quad n > 2 \quad (4.79)$$

The first few terms of x are shown:

$$x = t - \frac{8t^{\frac{5}{2}}}{15\sqrt{\pi}} + \frac{t^4}{24} - \frac{64t^{\frac{11}{2}}}{10395\sqrt{\pi}} + \frac{t^7}{5040} - \frac{512t^{\frac{17}{2}}}{34459425\sqrt{\pi}} + \frac{t^{10}}{3628800} + \dots \quad (4.80)$$

Approximately 30 non-zero C_n coefficients of the series solution are generated using the maxima code given in appendix A.2 and plotted in Fig.4.2. Plotting this truncated power series solution and comparing with the solution of the Laplace method, Fig.4.3, we find the two to be in good agreement.

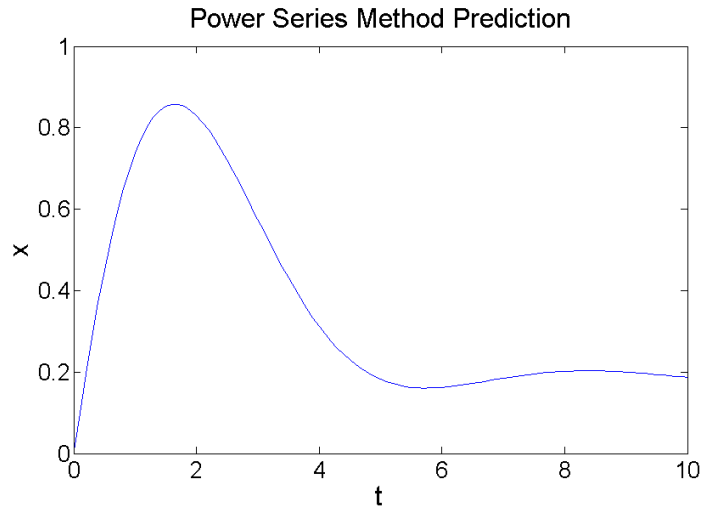


Figure 4.2: Solution to (4.31) given by (4.73) and (4.79) with $\mu = 1$, $\alpha = 1/2$, and $v = 2$ truncated to approximately 30 non-zero terms.

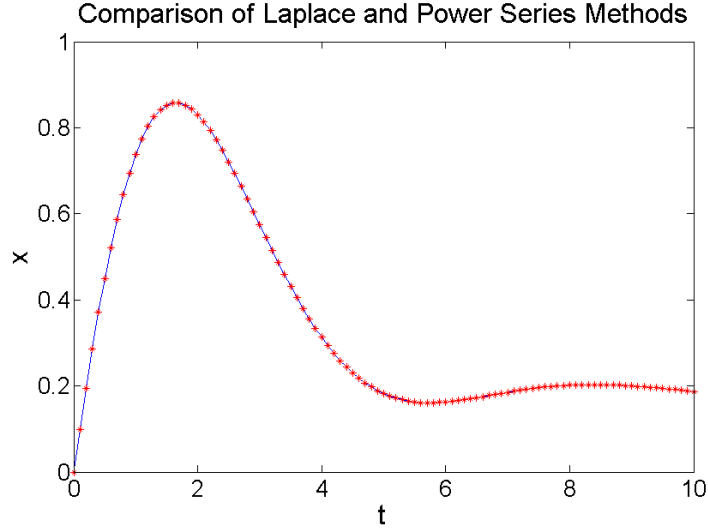


Figure 4.3: Comparison of solutions to (4.31) with $\mu = 1$ and $\alpha = 1/2$ predicted using the Laplace transform method and power series method. The Laplace solution given by (4.68) with (4.72) is shown by the solid line. The power series solution is given by (4.73) and (4.79) with $v = 2$ and truncated to approximately 30 non-zero terms and shown by the asterisks.

4.2.3 Numerical Solution

Calculating a numerical solution to a fractional differential equation requires significant computational effort due to the fractional derivative's dependence on the entire history of the function. To overcome this problem Podlubny [28] suggested a "short-memory" principle whereby the time history dependence is shortened to a chosen fixed length. Taking account of only the "recent past" can however lead to considerable inaccuracy and [11] instead presents a corrector approach method. Another obstacle in the numerical integration of a fractional derivative is the singularity present in the Riemann-Liouville integral representation at $v = 0$:

$$D^\alpha x(t) = \frac{1}{\Gamma(1-\alpha)} \int_0^t v^{-\alpha} x'(t-v) dv \quad (4.81)$$

In using the "short-memory" principle the singularity is avoided. It can alterna-

tively be avoided through a variable transformation as discussed in [23].

We utilize the simple Euler's method in our numerical integration algorithm with the fractional derivative, as defined by the Riemann-Liouville integral, computed using the trapezoid rule. Recall the system we are considering:

$$x'' + D^{1/2}x = 0 \tag{4.82}$$

Expressing (4.82) as a system of first order equations:

$$x' = y \tag{4.83}$$

$$y' = -D^{1/2}x \tag{4.84}$$

Uniformly discretizing the interval $t = nh$ where $n = 0, 1, 2, \dots$. Euler's method gives:

$$x_{n+1} = x_n + h y_n \tag{4.85}$$

$$y_{n+1} = y_n - h D_n^{1/2} x \tag{4.86}$$

The subscript n denotes that the variable is being evaluate at $t = nh$. The Riemann-Liouville integral expression (4.81) for the fractional derivative $D_n^{1/2}x$ is computed using the trapezoid rule. From (4.81):

$$D_n^{1/2}x = \frac{1}{\sqrt{\pi}} \int_0^{nh} z^{-1/2} x'(nh - z) dz \tag{4.87}$$

To avoid the singularity of the integrand at the lower bound of integration we first rewrite (4.87):

$$D_n^\alpha x = \frac{1}{\sqrt{\pi}} \left(\int_0^h z^{-\alpha} x'(nh - z) dz + \int_h^{nh} z^{-\alpha} x'(nh - z) dz \right) \quad (4.88)$$

We then approximate $z^{-\alpha}$ by $h^{-\alpha}$ in the first integral and evaluate.

$$D_n^\alpha x = \frac{1}{\sqrt{\pi}} \left(h^{-\alpha} (x_n - x_{n-1}) + \int_h^{nh} z^{-\alpha} x'(nh - z) dz \right) \quad (4.89)$$

The second integral may now be computed using the trapezoid rule with z taking on the same uniformly distributed values of t used in applying Euler's method.

$$D_n^\alpha x = \frac{1}{\Gamma(1-\alpha)} \left(h^{-\alpha} (x_n - x_{n-1}) + \frac{h}{2} \left(h^{-\alpha} x'_{n-1} + (nh)^{-\alpha} x'_0 + \sum_{m=2}^{n-1} 2 (mh)^{-\alpha} x'_{n-m} \right) \right) \quad (4.90)$$

$$= \frac{1}{\Gamma(1-\alpha)} \left(h^{-\alpha} (x_n - x_{n-1}) + \frac{h}{2} \left(h^{-\alpha} y_{n-1} + (nh)^{-\alpha} y_0 + \sum_{m=2}^{n-1} 2 (mh)^{-\alpha} y_{n-m} \right) \right) \quad (4.91)$$

This summation will have to be calculated at each time step to then be used in (4.86). The sum is also growing at each step and to ease the computation time it can be written as a vector inner product, where the two vectors will be updated at each step.

$$h^{-\alpha} y_{n-1} + \sum_{m=2}^{n-1} 2 (mh)^{-\alpha} y_{n-m} + (nh)^{-\alpha} y_0 = \bar{m}_{1_n} \bullet \bar{m}_{2_n} \quad (4.92)$$

$$\bar{m}_{1_n} = [h^{-\alpha}, 2(2h)^{-\alpha}, \dots, 2((n-1)h)^{-\alpha}, (nh)^{-\alpha}], \quad \bar{m}_{2_n} = [y_{n-1}, y_{n-2}, \dots, y_0] \quad (4.93)$$

$$\bar{m}_{1_{n+1}} = [\bar{m}_{1_n}(1 : n - 1), 2(nh)^{-\alpha}, ((n + 1)h)^{-\alpha}], \quad \bar{m}_{2_{n+1}} = [v_{2_n}, \bar{m}_{2_n}] \quad (4.94)$$

This recursive formula is implemented in Matlab and the program is given in appendix A.3 with the obtain solution plotted in Fig.4.4. The numerical solution is plotted against the Laplace solution and the two are shown to be in good agreement.

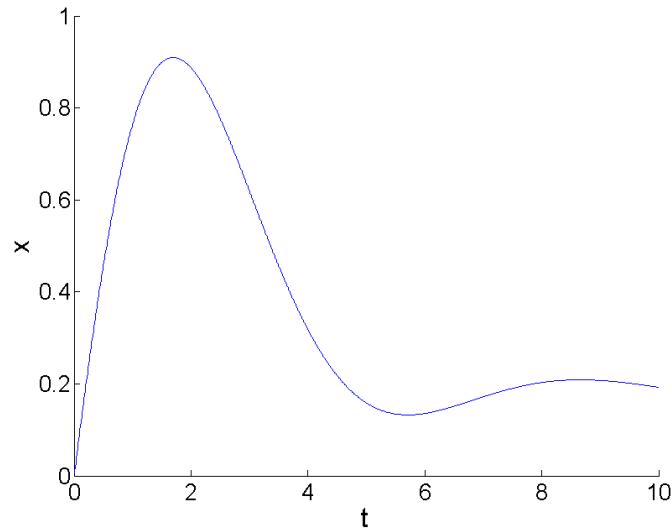


Figure 4.4: Solution obtain by numerically integrating (4.31) with $\mu = 1$ and $\alpha = 1/2$.

Integrating to $t = 100$ our intuition of the problem is verified as we see that the solution is decaying to zero, Fig.4.6. The numerical integration scheme outlined in this section will again be used in Chapter 6 where a pair of fractionally coupled van der Pol oscillators is considered.

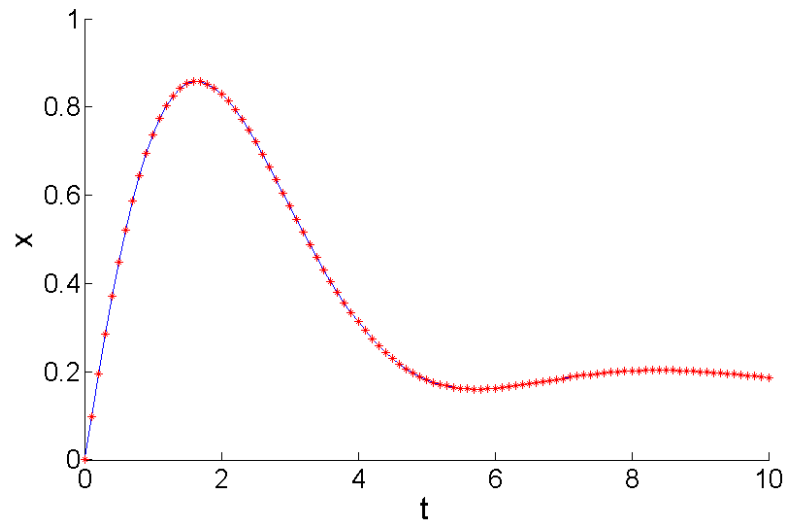


Figure 4.5: Comparison of numerical solution to (4.31) with $\mu = 1$ and $\alpha = 1/2$, shown as a solid line and solution found using the Laplace transform method shown with asterisks.

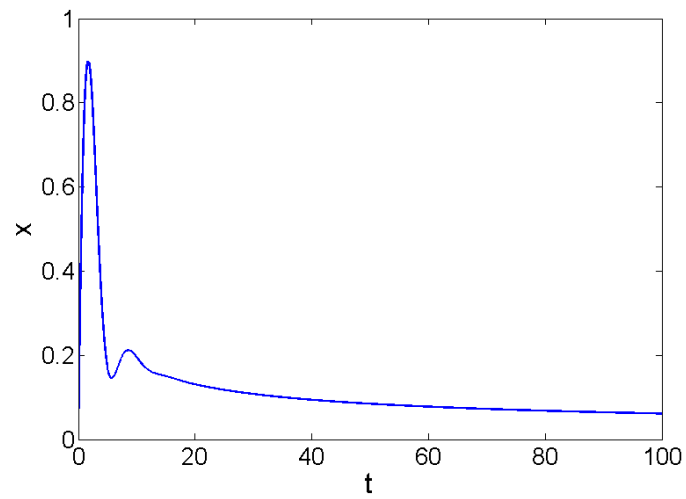


Figure 4.6: Numerical integration of (4.31) with $\mu = 1$ and $\alpha = 1/2$.

CHAPTER 5

FRACTIONAL MATHIEU EQUATION [33]

In this chapter we look to extend the treatment of Mathieu's equation:

$$x'' + (\delta + \epsilon \cos t)x = 0, \quad (5.1)$$

being an equation which is important in questions of stability of motion as well as in systems which are parametrically excited, to include the effect of a fractional derivative term:

$$x'' + (\delta + \epsilon \cos t)x + cD^\alpha x = 0 \quad (5.2)$$

In the case that $\alpha = 1$, eq.(5.2) represents the familiar damped Mathieu equation [31].

5.1 Mathieu's Equation

In this section we present a brief summary of the (non-fractional) Mathieu's equation (5.1) in order to assess the effects due to the addition of a fractional derivative term as in eq.(5.2). See e.g. Stoker [40]. For given values of the parameters δ and ϵ , either all solutions of Mathieu's equation are bounded (stable) or unbounded (unstable). The $\delta - \epsilon$ parameter plane is thus divided into stable and unstable regions. Although an infinite number of "resonance tongues" emerge from the δ -axis at $\delta = n^2/4$, where $n = 1, 2, 3, \dots$, most of these are insignificant for small values of ϵ , see Fig.5.1. This is not the case for the tongue emanating from $\delta = 1/4$, which is important in applications and is associated with 2:1 subharmonic resonance. From perturbation theory it is known [31] that this tongue has the following asymptotic

expansion:

$$\delta = \frac{1}{4} \pm \frac{1}{2}\epsilon - \frac{1}{8}\epsilon^2 + O(\epsilon^3) \quad (5.3)$$

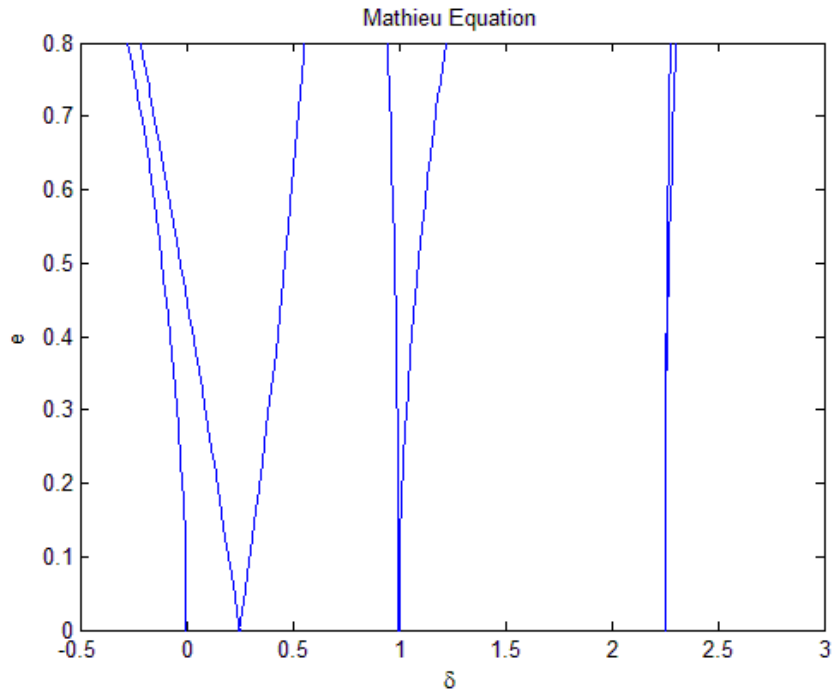


Figure 5.1: Transition curves in Mathieu's equation (5.1). Displayed are eqs.(5.3),(5.4) as well as other curves whose equations are not listed here. See [31].

In addition to the aforementioned tongues, there is also a transition curve separating stable from unstable regions emanating from the origin in the $\delta - \epsilon$ plane.

It has the following expansion:

$$\delta = -\frac{1}{2}\epsilon^2 + \frac{7}{32}\epsilon^4 + O(\epsilon^6) \quad (5.4)$$

If a damping term is added, we obtain the damped Mathieu equation:

$$x'' + (\delta + \epsilon \cos t)x + cx' = 0 \quad (5.5)$$

The effect of the damping term on the shape of the transition curves is to detach each of the tongues from the δ -axis, thereby requiring a minimum value of ϵ for

instability to occur [31]. In the case of the $n = 1$ tongue, eq.(5.5) has the following expansion, see Fig.5.2:

$$\delta = \frac{1}{4} \pm \frac{1}{2} \sqrt{\epsilon^2 - c^2} + O(\epsilon^3) \quad (5.6)$$

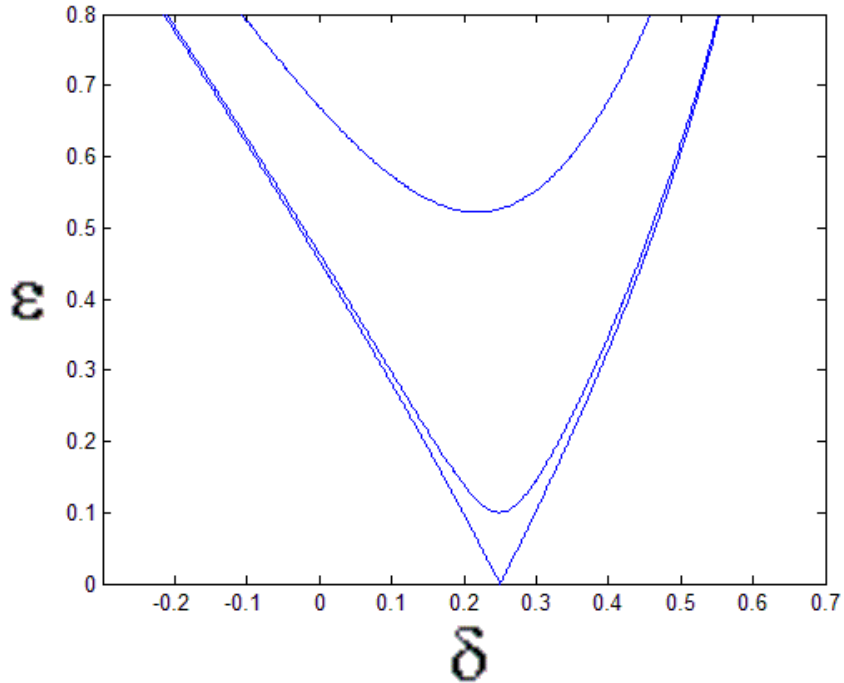


Figure 5.2: Transition curves (5.6) in the damped Mathieu equation (5.5). The upper curve corresponds to $c = 0.5$. The middle curve corresponds to $c = 0.1$. The lower curve corresponds to $c = 0$.

5.2 Transition curves of the fractional Mathieu equation

In this section we use the method of harmonic balance to obtain approximate expressions for the transition curves in the fractional Mathieu equation:

$$x'' + (\delta + \epsilon \cos t)x + cD^\alpha x = 0 \quad (5.7)$$

From Floquet theory [31] it is known that on the transition curves there exist periodic solutions to (5.7) with period 2π or 4π . Thus in order to obtain an

approximation for the $n = 1$ transition curves, we posit a truncated Fourier series:

$$x = A \cos \frac{t}{2} + B \sin \frac{t}{2} + \dots \quad (5.8)$$

In substituting (5.8) into (5.7) we need to compute the fractional derivative $D^\alpha x$, where $0 < \alpha < 1$, which we do by using the definition (4.27):

$$D^\alpha x = \frac{1}{\Gamma(1-\alpha)} \int_0^t v^{-\alpha} x'(t-v) dv \quad (5.9)$$

$$\int_0^t v^{-\alpha} x'(t-v) dv = \frac{1}{2} \int_0^t v^{-\alpha} \left(-A \sin \frac{t-v}{2} + B \cos \frac{t-v}{2} \right) dv \quad (5.10)$$

Here we use the trig identities:

$$\cos \frac{t-v}{2} = \cos \frac{t}{2} \cos \frac{v}{2} + \sin \frac{t}{2} \sin \frac{v}{2} \quad (5.11)$$

$$\sin \frac{t-v}{2} = \sin \frac{t}{2} \cos \frac{v}{2} - \cos \frac{t}{2} \sin \frac{v}{2} \quad (5.12)$$

and eq.(5.10) becomes

$$\begin{aligned} \int_0^t v^{-\alpha} x'(t-v) dv &= \frac{1}{2} \cos \frac{t}{2} \int_0^t v^{-\alpha} \left(B \cos \frac{v}{2} + A \sin \frac{v}{2} \right) dv \\ &\quad + \frac{1}{2} \sin \frac{t}{2} \int_0^t v^{-\alpha} \left(B \sin \frac{v}{2} - A \cos \frac{v}{2} \right) dv \end{aligned} \quad (5.13)$$

$$= \frac{1}{2^\alpha} \cos \frac{t}{2} (BI_c + AI_s) + \frac{1}{2^\alpha} \sin \frac{t}{2} (-AI_c + BI_s) \quad (5.14)$$

where

$$I_c = \int_0^{t/2} w^{-\alpha} \cos w dw \quad \text{and} \quad I_s = \int_0^{t/2} w^{-\alpha} \sin w dw \quad (5.15)$$

Although these integrals cannot be evaluated in closed form for general values of t , maxima is able to evaluate them in the limit as $t \rightarrow \infty$:

$$\int_0^\infty w^{-\alpha} \cos w dw = \Gamma(1-\alpha) \sin \frac{\alpha\pi}{2} \quad \text{and} \quad \int_0^\infty w^{-\alpha} \sin w dw = \Gamma(1-\alpha) \cos \frac{\alpha\pi}{2} \quad (5.16)$$

After [49],[47] we approximate I_c and I_s in eqs.(5.14),(5.15) by their values in eqs.(5.16) in what follows, thereby restricting attention to the large t limit. Thus we find from eq.(5.9) the following expression for the fractional derivative:

$$D^\alpha x = \frac{1}{2^\alpha} \cos \frac{t}{2} \left(B \sin \frac{\alpha\pi}{2} + A \cos \frac{\alpha\pi}{2} \right) + \frac{1}{2^\alpha} \sin \frac{t}{2} \left(-A \sin \frac{\alpha\pi}{2} + B \cos \frac{\alpha\pi}{2} \right) \quad (5.17)$$

Next we substitute (5.8) and (5.17) into (5.7) and collect terms, equating to zero coefficients of $\sin \frac{t}{2}$ and $\cos \frac{t}{2}$. Eliminating A and B from the resulting two equations gives the following approximate expression for the $n = 1$ transition curves:

$$\delta = \frac{1}{4} - \frac{c}{2^\alpha} \cos \frac{\alpha\pi}{2} \pm \frac{\sqrt{2^{2\alpha} \epsilon^2 - 4c^2 \sin^2 \frac{\alpha\pi}{2}}}{2^{\alpha+1}} \quad (5.18)$$

As a check, we substitute $\alpha = 1$ in eq.(5.18), in which case the fractional derivative in eq.(5.7) becomes an ordinary first derivative and we obtain eq.(5.6) corresponding to the damped Mathieu equation (5.5). Fig.5.3 displays the transition curves (5.18) for various values of α .

We may obtain a higher order approximation by replacing the original ansatz (5.8) by the following:

$$x = A \cos \frac{t}{2} + B \sin \frac{t}{2} + G \cos \frac{3t}{2} + H \sin \frac{3t}{2} + \dots \quad (5.19)$$

Proceeding as before we obtain an algebraic equation relating δ , ϵ and α which is too complicated to list here. See Fig.5.4 where it is displayed along with eq.(5.18) for $\alpha = 1/2$.

In a similar fashion we may obtain approximations for the other transition curves. For example, in order to obtain an expression for the $n = 0$ transition curve which passes through the origin in the $\delta - \epsilon$ plane, we start with the ansatz:

$$x = A \cos t + B \sin t + G + \dots \quad (5.20)$$

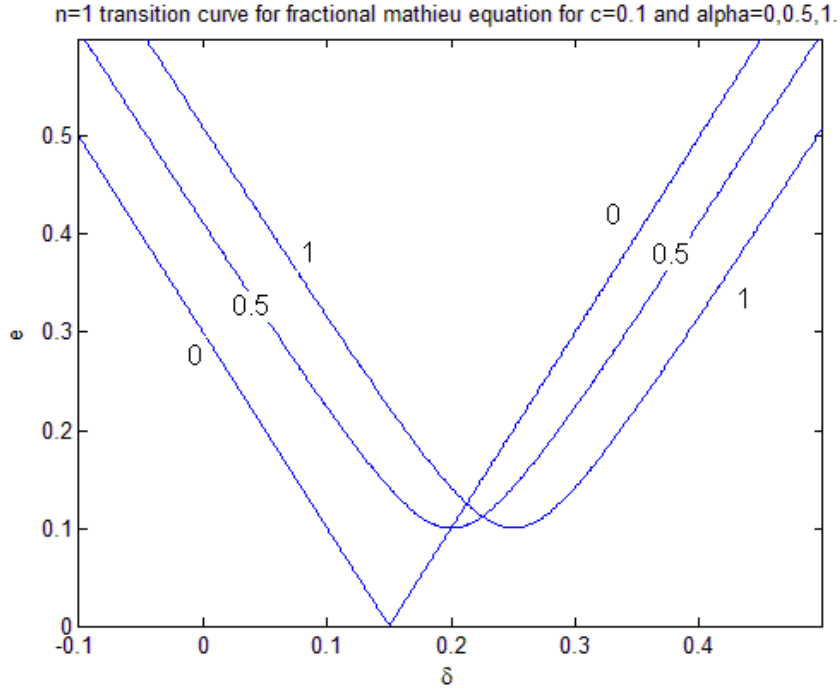


Figure 5.3: $n = 1$ transition curve, eq.(5.18), in the fractional Mathieu equation (5.7) for $c = 0.1$ and $\alpha = 0, 0.5, 1$.

Proceeding as before we obtain the following expression for the $n = 0$ transition curve:

$$(Kc - 1)\epsilon^2 + (\epsilon^2 - 2c^2 + 4Kc - 2)\delta + 4(1 - Kc)\delta^2 - 2\delta^3 = 0 \quad (5.21)$$

where $K = \cos \frac{\alpha\pi}{2}$. Fig.5.5 shows the $n = 0$ transition curve for various values of α . We note that the shape of the transition curve does not change very much for α in the range $[0,1]$.

5.3 Discussion

In the case of the $n = 1$ transition curves (see eq.(5.18) and .5.3), we see that a change in the order α of the fractional derivative affects the shape and location of

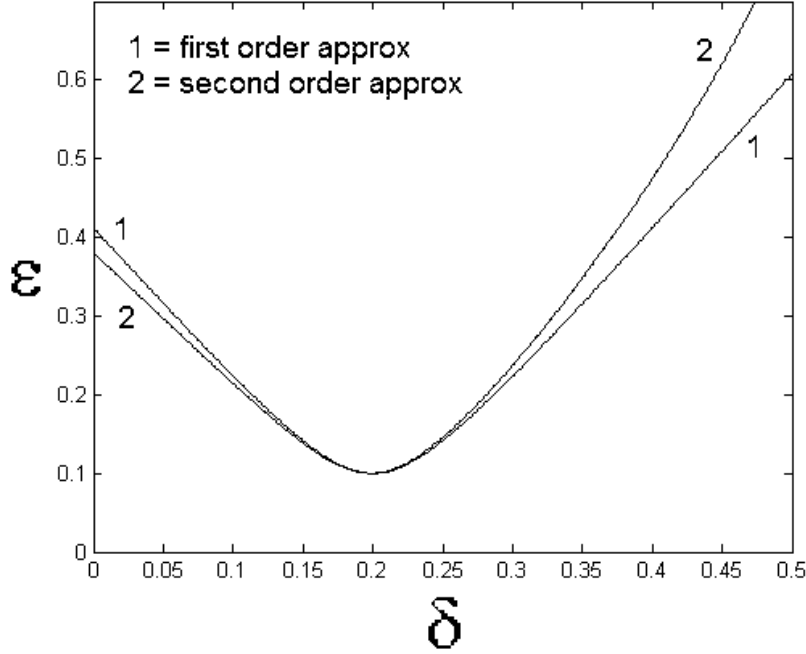


Figure 5.4: $n=1$ transition curves in the fractional Mathieu equation (5.7) for $\alpha = 0.5$ and $c = 0.1$. First and second order approximations, as obtained by the method of harmonic balance. The first order approximation is given by eq.(5.18). The second order approximation has 51 terms and is too long to list here.

the transition curves. This effect can be characterized by the location of the lowest point on the transition curve, which represents the minimum quantity of forcing amplitude ϵ necessary to produce instability. Let us refer to this minimum value of ϵ , for a given value of α , as ϵ_{min} . See Fig.5.6, where eq.(5.18) is displayed as a surface in $\delta - \epsilon - \alpha$ space.

In order to obtain an expression for ϵ_{min} , we may differentiate eq.(5.18) with respect to ϵ , giving the slope of the transition curve, and require this slope to be infinite. We find:

$$\epsilon_{min} = 2c \left(\frac{\sin \frac{\alpha\pi}{2}}{2^\alpha} \right) \quad (5.22)$$

See Fig.5.7, where ϵ_{min} is plotted as a function of α . The greatest effect is observed

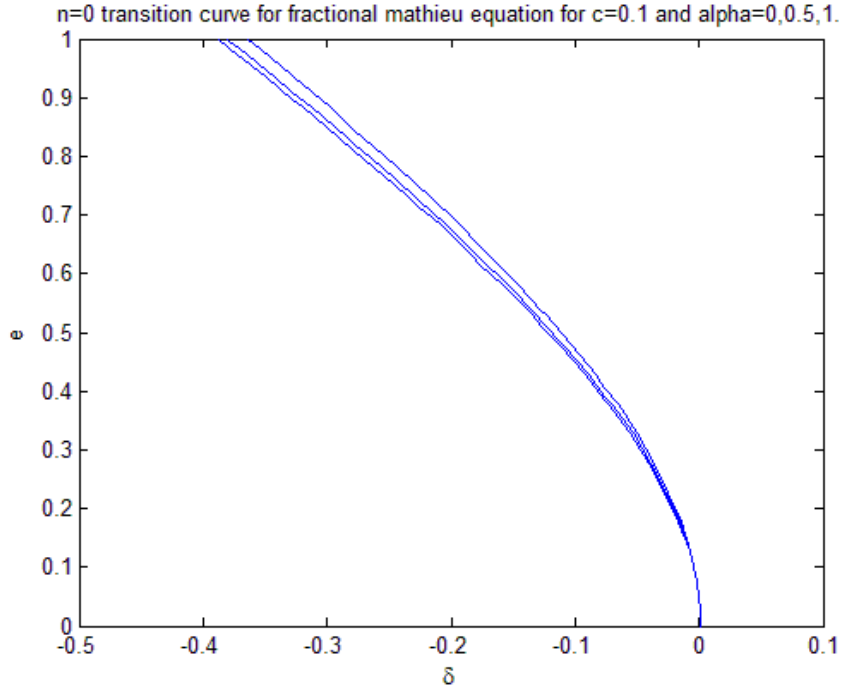


Figure 5.5: $n = 0$ transition curve, eq.(5.21), in the fractional Mathieu equation (5.7) for $c = 0.1$ and $\alpha = 0, 0.5, 1$. The leftmost curve corresponds to $\alpha = 0$. The middle curve corresponds to $\alpha = 0.5$. The rightmost curve corresponds to $\alpha = 1$.

where this curve achieves its maximum, shown by a dot in Fig.7. Let us refer to the corresponding value of α as α^* . Then we may obtain an expression for α^* by differentiating eq.(5.22) with respect to α and setting $d\epsilon_{min}/d\alpha$ equal to zero. We find:

$$\alpha^* = \frac{2}{\pi} \arctan \frac{\pi}{2} \approx 0.735 \quad (5.23)$$

Let us refer to the corresponding value of ϵ_{min} as ϵ_{min}^* . We find:

$$\epsilon_{min}^* \approx 1.099c \quad (5.24)$$

This effect is reminiscent of the (non-fractional) damped Mathieu eq.(5.5), cf.Fig.2, which corresponds here to $\alpha = 1$. Note from Fig.7, that when α lies in the range $(0.5,1)$, the values for ϵ_{min} are all greater than ϵ_{min} for eq.(5.5). Thus we may say that the damping effect of the fractional derivative term in eq.(5.7), for $0.5 < \alpha < 1$,

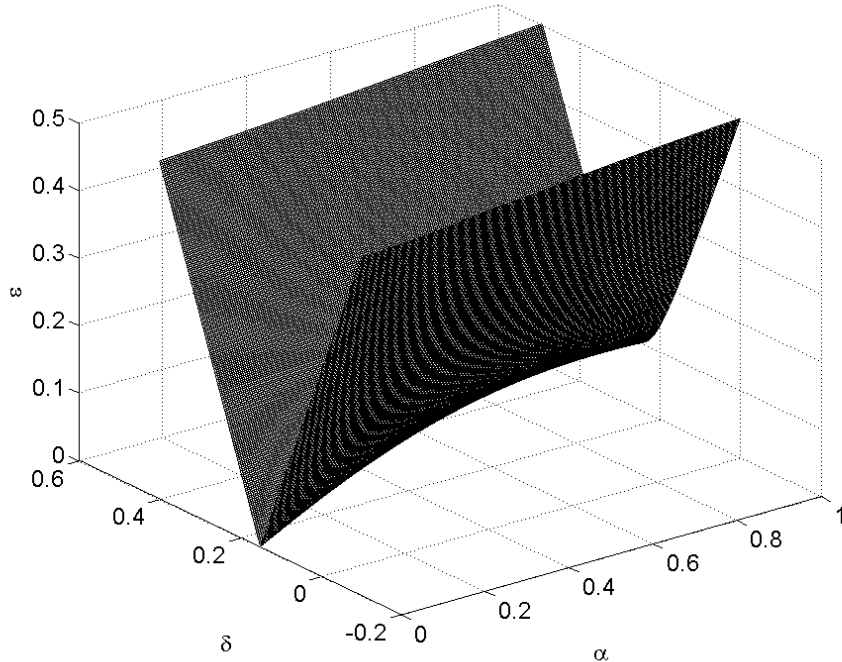


Figure 5.6: Eq.(5.18) displayed in $\delta - \epsilon - \alpha$ space for $c = 0.1$

is greater than that of the (non-fractional) damped Mathieu eq.(5.5).

Note also that in contrast to non-fractional damping, fractional damping also moves this lowest point on the transition curve in a horizontal direction, see Fig.3, thereby effectively changing the resonant value of δ .

On the other hand, in the case of the $n = 0$ transition curves (see eq.(5.21) and Fig.5), we see that there is very little change as α is varied.

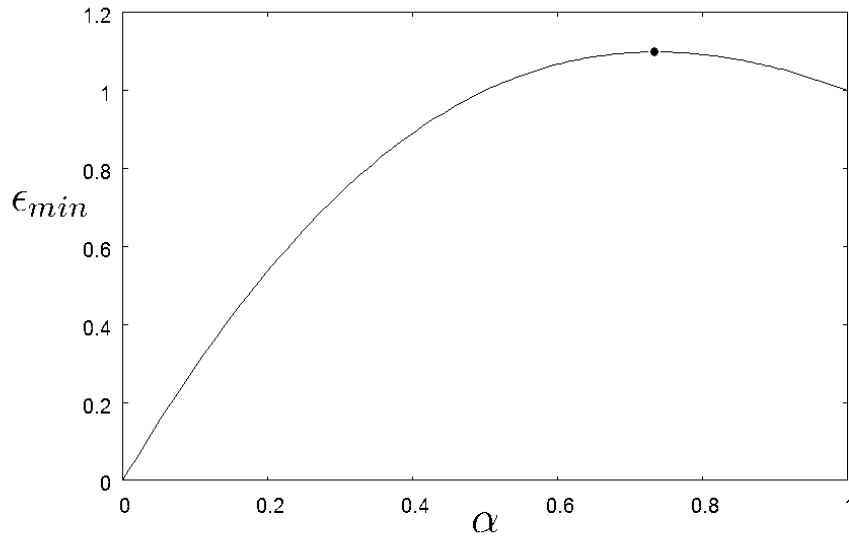


Figure 5.7: Plot of ϵ_{min} , the minimum quantity of forcing amplitude ϵ necessary to produce instability, as a function of fractional derivative order α , eq.(5.22). The greatest effect is observed where this curve achieves its maximum, shown as a dot here, and referred to as α^* in the text.

5.4 Summary

The method of harmonic balance was used to obtain explicit approximate expressions for the $n = 1$ and $n = 0$ transition curves separating regions of stability from regions of instability in the fractional Mathieu equation (5.7). We showed that by changing the value of the order of the fractional derivative, α , the shape and location of the $n = 1$ transition curve can be changed. In particular we showed that the minimum quantity of forcing amplitude ϵ necessary to produce instability was greatest for $\alpha^* \approx 0.735$.

CHAPTER 6

A PAIR OF VAN DER POLS COUPLED WITH FRACTIONAL DERIVATIVES [44]

In this chapter we look to extend the treatment of a pair of coupled van der Pol oscillators. Previous works [41], [29] have considered the stability of the in-phase and out-of-phase modes of a system of van der Pol oscillator with varying types of coupling. Consider the system investigated by [41] where two van der Pol oscillators are connected through both position-coupling and velocity-coupling terms.

$$x'' - \epsilon(1 - x^2)x' + x = \epsilon A(y - x) + \epsilon B(y' - x') \quad (6.1)$$

$$y'' - \epsilon(1 - y^2)y' + y = \epsilon A(x - y) + \epsilon B(x' - y') \quad (6.2)$$

We instead consider the case of fractional-coupling:

$$x'' - \epsilon(1 - x^2)x' + x = \epsilon \gamma D^\alpha(y - x) \quad (6.3)$$

$$y'' - \epsilon(1 - y^2)y' + y = \epsilon \gamma D^\alpha(x - y) \quad (6.4)$$

In the limits of $\alpha \rightarrow 0$ and $\alpha \rightarrow 1$ the fractional-coupling respectively reduces to position-coupling and velocity coupling. We look for the convergence of our results with those of previous works in these limiting cases of α .

We begin the chapter with a brief introduction to the fractional calculus. See e.g. [25],[36],[28],[20],[39].

6.1 Stability of the in-phase mode

The system under consideration is composed of two van der Pol oscillators coupled by the fractional derivatives of their positions.

$$x'' - \epsilon(1 - x^2) x' + x = \epsilon \gamma D^\alpha (y - x) \quad (6.5)$$

$$y'' - \epsilon(1 - y^2) y' + y = \epsilon \gamma D^\alpha (x - y) \quad (6.6)$$

There exists an in-phase manifold defined by $x = y$. On this manifold the coupling term vanishes and the system is reduced to two identical van der pol oscillators. An approximate solution for this mode exists and is the limit cycle of the uncoupled van der Pol equation. To determine the stability of the in-phase mode we look at small disturbances from it. The variational equations govern the evolution of these small disturbances. To obtain the variational equations we introduce the small deviations $\phi = x - u$ and $\psi = y - u$ where u is the in-phase mode $u(t) = x(t) = y(t)$. Substituting these expressions into (6.5)-(6.6) and ignoring nonlinear terms yields:

$$\phi'' - \epsilon(1 - u^2) \phi' + (1 + 2\epsilon u u') \phi = \epsilon \gamma D^\alpha (\psi - \phi) \quad (6.7)$$

$$\psi'' - \epsilon(1 - u^2) \psi' + (1 + 2\epsilon u u') \psi = \epsilon \gamma D^\alpha (\phi - \psi) \quad (6.8)$$

Defining the quantities $w = \phi + \psi$ and $v = \phi - \psi$ uncouples these equations.

$$w'' - \epsilon(1 - u^2) w' + (1 + \epsilon 2 u u') w = 0 \quad (6.9)$$

$$v'' - \epsilon(1 - u^2) v' + (1 + \epsilon 2 u u') v = -2\epsilon\gamma D^\alpha v \quad (6.10)$$

Observe that (6.9) is also the variational equation corresponding to a single van der Pol oscillator, meaning that it is obtained when one considers a small deviation from the limit cycle of the van der Pol equation. This then implies that within our system of fractionally-coupled van der Pols, (6.9) governs deviations from the in-phase mode that themselves lie on the in-phase manifold. Since the limit cycle of the van der Pol equation is known to be orbitally stable, we follow [41] and conclude that (6.9) does not cause instability of the in-phase solution within our coupled system.

Equation (6.10) governs deviations transverse to the in-phase manifold. We examine whether this type of deviation will cause instability by employing a two variable perturbation method. We begin the perturbation method by defining:

$$\xi = \omega t, \quad \eta = \epsilon t \quad (6.11)$$

where ω is the power series expansion in ϵ for the frequency of the van der Pol's limit cycle as given by eq.(16) in Storti [41]:

$$\omega = 1 + O(\epsilon^2) \quad (6.12)$$

By the chain rule the quantities v' and v'' become:

$$v' = \omega v_\xi + \epsilon v_\eta \quad (6.13)$$

$$v'' = \omega^2 v_{\xi\xi} + 2\omega\epsilon v_{\xi\eta} + \epsilon^2 v_{\eta\eta} \quad (6.14)$$

Recalling (4.27) for $0 < \alpha < 1$ the fractional derivative is defined as:

$$D^\alpha x(t) = \frac{1}{\Gamma(1-\alpha)} \int_0^t z^{-\alpha} x'(t-z) dz \quad (6.15)$$

Osler [26] has shown that for a function of the form $x(\xi)$ where $\xi = \omega t$:

$$D_t^\alpha x(\xi) = \omega^\alpha D_\xi^\alpha x(\xi) \quad (6.16)$$

We assume that for functions of two arguments $x(\xi, \eta)$ where $\eta = \epsilon t$:

$$D_t^\alpha x(\xi, \eta) = \omega^\alpha D_\xi^\alpha x(\xi, \eta) + o(1) \quad (6.17)$$

$$= \frac{\omega^\alpha}{\Gamma(1-\alpha)} \int_0^\xi z^{-\alpha} x_\xi(\xi-z, \eta) dz + o(1) \quad (6.18)$$

From (6.12)-(6.14) and (6.18), in terms of ξ and η , (6.10) becomes:

$$v_{\xi\xi} + 2\epsilon v_{\xi\eta} - \epsilon(1-u^2)v_\xi + (1+2\epsilon u u_\xi)v + O(\epsilon^2) = -2\epsilon\gamma \frac{1}{\Gamma(1-\alpha)} \int_0^\xi z^{-\alpha} x_\xi(\xi-z, \eta) dz + o(\epsilon) \quad (6.19)$$

The in-phase mode, the van der Pol limit cycle, can be approximated by power series in ϵ .

$$u = 2 \cos \xi + O(\epsilon) \quad (6.20)$$

We posit a power series solution for v :

$$v(\xi, \eta) = v_0(\xi, \eta) + \epsilon v_1(\xi, \eta) + \dots \quad (6.21)$$

Substituting these two power series expressions (6.20)-(6.21) into (6.19) and collecting terms we obtain:

$$O(1) : \mathcal{L}v_0 = 0 \quad (6.22)$$

$$O(\epsilon) : \mathcal{L}v_1 = -2v_{0\xi\eta} - (1 + 2 \cos \xi)v_{0\xi} + (4 \sin 2\xi)v - 2\gamma D_\xi^\alpha v_0 \quad (6.23)$$

Where \mathcal{L} is the linear operator, $\mathcal{L}v_0 = v_{0\xi\xi} + v_0$. The general solution to (6.22) is given by:

$$v_0 = A(\eta) \cos \xi + B(\eta) \sin \xi \quad (6.24)$$

This general solution is substituted into the $O(\epsilon)$ equation (6.23) and resonant terms are identified. The nonresonant terms are noted as NRT.

$$\mathcal{L}v_1 = 2A \sin \xi + 2A' \sin \xi - 2B' \cos \xi - 2\gamma D_\xi^\alpha (A(\eta) \cos \xi + B(\eta) \sin \xi) + NRT \quad (6.25)$$

The fractional derivative (6.15) cannot be computed in closed form. Instead we approximate the fractional derivative by evaluating the integral in the limit as $\xi \rightarrow \infty$ and therefore expect our results to be valid for steady state [47], [49].

$$D_\xi^\alpha v_0(\xi, \eta) = \frac{1}{\Gamma(1-\alpha)} \int_0^\xi z^{-\alpha} (-A(\eta) \sin(\xi - z) + B(\eta) \cos(\xi - z)) dz \quad (6.26)$$

$$\begin{aligned} &= \frac{\cos \xi}{\Gamma(1-\alpha)} \int_0^\xi z^{-\alpha} (A(\eta) \sin z + B(\eta) \cos z) dz \\ &\quad + \frac{\sin \xi}{\Gamma(1-\alpha)} \int_0^\xi z^{-\alpha} (-A(\eta) \cos z + B(\eta) \sin z) dz \end{aligned} \quad (6.27)$$

$$= \frac{\cos \xi}{\Gamma(1-\alpha)} (A(\eta)I_s + B(\eta)I_c) + \frac{\sin \xi}{\Gamma(1-\alpha)} (-A(\eta)I_c + B(\eta)I_s) \quad (6.28)$$

where:

$$I_c = \int_0^\xi z^{-\alpha} \cos z dz, \quad I_s = \int_0^\xi z^{-\alpha} \sin z dz \quad (6.29)$$

In the limit as $t \rightarrow \infty$ these integrals become:

$$\int_0^\infty z^{-\alpha} \cos z dz = \Gamma(1-\alpha) \sin \frac{\alpha \pi}{2}, \quad \int_0^\infty z^{-\alpha} \sin z dz = \Gamma(1-\alpha) \cos \frac{\alpha \pi}{2} \quad (6.30)$$

Combining the results of (6.28)-(6.30) yields the final expression for our approximation to $D_\xi^\alpha v_0(\xi, \eta)$:

$$D_\xi^\alpha v_0(\xi, \eta) = \cos \xi \left(A(\eta) \cos \frac{\alpha \pi}{2} + B(\eta) \sin \frac{\alpha \pi}{2} \right) + \sin \xi \left(-A(\eta) \sin \frac{\alpha \pi}{2} + B(\eta) \cos \frac{\alpha \pi}{2} \right) \quad (6.31)$$

Applying (6.31) to (6.25) yields:

$$\begin{aligned} \mathcal{L}v_1 = & \left(2A + 2A' + 2\gamma \left(A \sin \frac{\alpha\pi}{2} - B \cos \frac{\alpha\pi}{2}\right)\right) \sin \xi \\ & + \left(-2B' - 2\gamma \left(A \cos \frac{\alpha\pi}{2} + B \sin \frac{\alpha\pi}{2}\right)\right) \cos \xi + NRT \end{aligned} \quad (6.32)$$

We obtain the slow flow equations by setting the secular terms to zero:

$$A' = \left(-1 - \gamma \sin \frac{\alpha\pi}{2}\right) A + \gamma B \cos \frac{\alpha\pi}{2} \quad (6.33)$$

$$B' = -\gamma A \cos \frac{\alpha\pi}{2} - \gamma B \sin \frac{\alpha\pi}{2} \quad (6.34)$$

This is a linear system of equations and can be written in matrix form:

$$\begin{bmatrix} A' \\ B' \end{bmatrix} = \begin{bmatrix} M \end{bmatrix} \begin{bmatrix} A \\ B \end{bmatrix} \quad (6.35)$$

with coefficient matrix:

$$M = \begin{bmatrix} -1 - \gamma \sin \frac{\alpha\pi}{2} & \gamma \cos \frac{\alpha\pi}{2} \\ -\gamma \cos \frac{\alpha\pi}{2} & -\gamma \sin \frac{\alpha\pi}{2} \end{bmatrix} \quad (6.36)$$

We categorize the stability of the system by analyzing the trace, tr , and determinant, det , of the coefficient matrix M .

$$tr = -1 - 2\gamma \sin \frac{\alpha\pi}{2} \quad (6.37)$$

$$det = \gamma \left(\gamma + \sin \frac{\alpha\pi}{2}\right) \quad (6.38)$$

There are two ways in which the system can change stability one when $det = 0$ with $tr < 0$, secondly when $tr = 0$ with $det > 0$ which corresponds to a Hopf bifurcation. The critical transition curves for stability $tr = 0$ and $det = 0$ are plotted in Fig.6.1 and the regions of stability and instability are found.

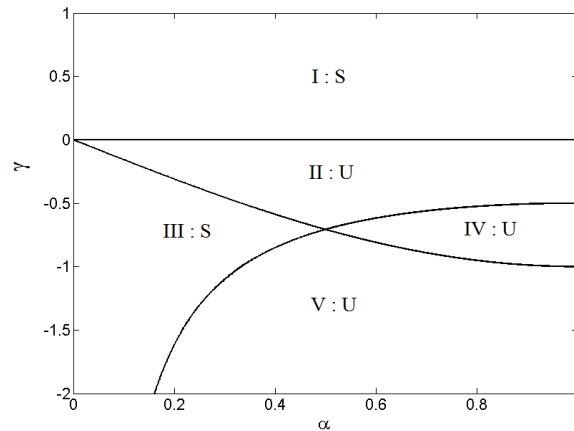


Figure 6.1: Stability of the in-phase mode as predicted by the perturbation method. S denotes stable and U unstable. Regions I and III are both stable and composed of nodes and foci. Regions II, IV and V are unstable. Regions II and IV are filled with saddles and region V is composed of unstable nodes and foci, cf. (6.37)-(6.38).

These results are checked by numerically integrating (6.10) with u given by (6.20) and $\epsilon = 0.1$. A large number of discrete points in the α vs. γ parameter space are chosen and the system is then integrated for each γ, α pair and checked for fulfillment of our chosen criterion for stability. The numerical integration is accomplished by following the algorithm outlined in section 4.2.3.

Both the perturbation method and numerical results are shown in Fig.6.2. The asterisks represent stable parameter values and the circles unstable. These results are in good agreement with our perturbation method's results previously shown in Fig.6.1 in that they both predict a stability change near the line $\gamma = 0$ as well as a wedge of stability in the $\gamma < 0$ region.

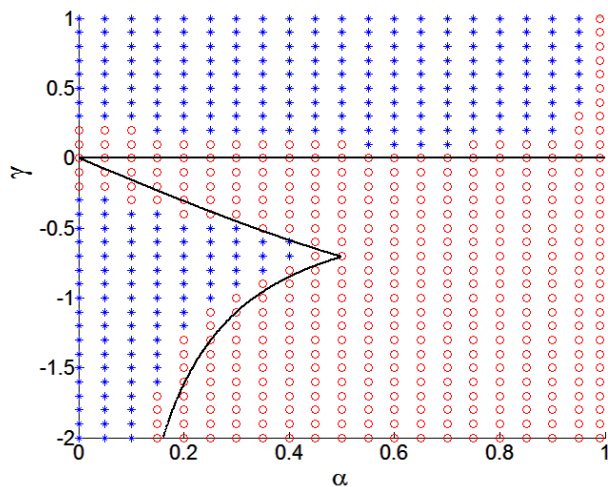


Figure 6.2: Comparison of perturbation method's stability results for the in-phase mode previously shown in Fig.6.1 with numerical integration of (6.10) with u given by (6.20) and ϵ taken as $\epsilon = .01$. The asterisks represent stable parameter values and the circles unstable.

Our results also agree with those of Storti and Reinhall [41] in the limiting cases of $\alpha = 0$ and $\alpha = 1$ which respectively correspond to position-coupling and velocity-coupling. In the case of $\alpha = 0$ we find the in-phase mode to be stable for all values of the coupling coefficient. However note that "all values" is taken to mean all values for which the perturbation method is valid and therefore can reasonably be classified as coefficients of $O(1)$. This agrees with [41] where they find a loss of stability at a coupling coefficient of $-0.5/\epsilon$ which is beyond the scope of our perturbation method. For the case of $\alpha = 1$ our results agree with [41] in that stability of the in-phase mode is lost as the coupling coefficient transitions from a positive value to a negative one.

6.2 Stability of the out-of-phase mode

Next we consider the stability of the out-of-phase mode. The out-of-phase mode is characterized by the motions where $x = -y = q$. Substituting $x = -y = q$ into each of our coupled van der Pol equations, (6.5) and (6.6), they admit identical equations. This one equation, (6.39), must therefore be satisfied for the out-of-phase mode to exist:

$$q'' - \epsilon(1 - q^2)q' + q = -2\epsilon\gamma D^\alpha q \quad (6.39)$$

We seek to determine for which values of parameters γ and α will (6.39) exhibit periodic motions. A two variable expansion is applied to answer this question. Periodic solutions can then be identified as fixed points in the slow flow equations produced from applying this perturbation method. Mirroring our in-phase analysis we begin by again defining:

$$\xi = \omega t, \quad \eta = \epsilon t \quad (6.40)$$

where ω is the power series expansion:

$$\omega = 1 + O(\epsilon^2) \quad (6.41)$$

By the chain rule q' and q'' become:

$$q' = \omega q_\xi + \epsilon q_\eta \quad (6.42)$$

$$q'' = \omega^2 q_{\xi\xi} + 2\omega\epsilon q_{\xi\eta} + \epsilon^2 q_{\eta\eta} \quad (6.43)$$

Recall that from (6.17) with (6.41) the fractional derivative is given by:

$$D_t^\alpha q(\xi, \eta) = D_\xi^\alpha q(\xi, \eta) + o(1) \quad (6.44)$$

We posit a power series solution for q :

$$q(\xi, \eta) = q_0(\xi, \eta) + \epsilon q_1(\xi, \eta) + O(\epsilon^2) \quad (6.45)$$

Substituting (6.42)-(6.44) into the equation governing the out-of-phase motion (6.39) and collecting terms we obtain:

$$O(1) : \mathcal{L}q_0 = 0 \quad (6.46)$$

$$O(\epsilon) : \mathcal{L}q_1 = -2q_{0\xi\eta} + (1 - q_0^2)q_{0\xi} - 2\gamma D_\xi^\alpha q_0 \quad (6.47)$$

Where \mathcal{L} is the linear operator, $\mathcal{L}q_0 = q_{0\xi\xi} + q_0$. The general solution to (6.46) is given by:

$$q_0 = A(\eta) \cos \xi + B(\eta) \sin \xi \quad (6.48)$$

Substituting this general solution into the $O(\epsilon)$ equation (6.47) we collect the resonant terms and identify nonresonant terms as NRT:

$$\begin{aligned} \mathcal{L}v_1 = & \sin \xi \left(\frac{AB^2}{4} + 2A' + \frac{A^3}{4} - A \right) + \cos \xi \left(-2B' - \frac{B^3}{4} - \frac{A^2B}{4} + B \right) \\ & - 2\gamma D_\xi^\alpha (A(\eta) \cos \xi + B(\eta) \sin \xi) + NRT \end{aligned} \quad (6.49)$$

Recall our approximation for the fractional derivative (6.31):

$$D_\xi^\alpha q_0(\xi, \eta) = \cos \xi \left(A(\eta) \cos \frac{\alpha \pi}{2} + B(\eta) \sin \frac{\alpha \pi}{2} \right) + \sin \xi \left(-A(\eta) \sin \frac{\alpha \pi}{2} + B(\eta) \cos \frac{\alpha \pi}{2} \right) \quad (6.50)$$

Substituting this expression into (6.49), the resonant terms are collected and set to zero to obtain the slow flow equations:

$$A' = -\frac{AB^2}{8} - \frac{A^3}{8} + \frac{A}{2} - \gamma A \sin \frac{\alpha \pi}{2} + \gamma B \cos \frac{\alpha \pi}{2} \quad (6.51)$$

$$B' = -\frac{A^2B}{8} - \frac{B^3}{8} + \frac{B}{2} - \gamma B \sin \frac{\alpha \pi}{2} - \gamma A \cos \frac{\alpha \pi}{2} \quad (6.52)$$

To uncouple the slow flow equations we transform to polar coordinates:

$$q_0 = R(\eta) \cos(t - \theta(\eta)) \quad (6.53)$$

$$R' = -\frac{R^3 + R(8\gamma \sin \frac{\alpha \pi}{2} - 4)}{8} \quad (6.54)$$

$$\theta' = -\gamma \cos \frac{\alpha \pi}{2} \quad (6.55)$$

Since θ' equals a constant it will not change the periodic nature of q_0 in (6.53) but it will alter the period. Periodic solutions are then seen to correspond to fixed

points in the R slow flow equation. Solving $R' = 0$ for the amplitude R of these periodic solutions yields:

$$R = 2 \left(1 - 2\gamma \sin \frac{\alpha\pi}{2} \right)^{1/2} \quad (6.56)$$

This amplitude and hence the out-of-phase solution will exist for parameter γ and α pairs satisfying:

$$1 - 2\gamma \sin \frac{\alpha\pi}{2} > 0 \quad (6.57)$$

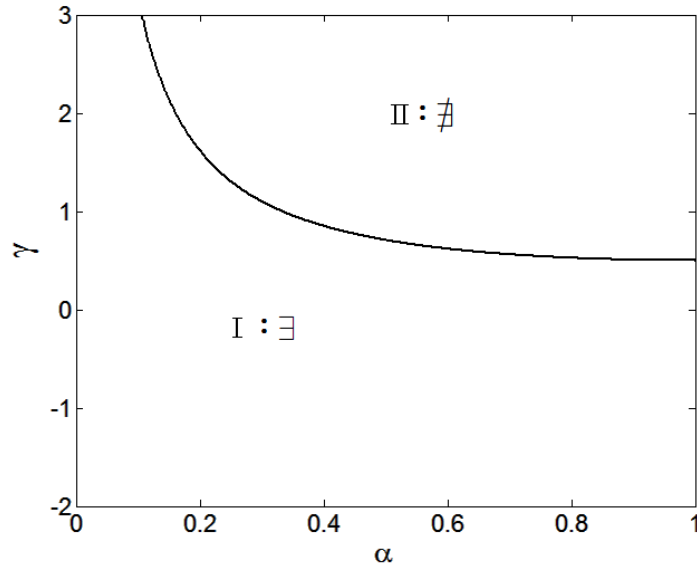


Figure 6.3: The perturbation method predicts the out-of-phase mode to exist only in region I as denoted by \exists cf. eq.(6.57). The out-of-phase mode doesn't exist in region II as noted in figure by \nexists symbol.

This result is shown in Fig.6.3 with the parameter plane divided into two regions where in each region the out-of-phase mode either exists or does not exist and the transition curve is given by $\sin \frac{\alpha\pi}{2} = \frac{1}{2\gamma}$ cf. eq.(6.57). This out-of-phase mode existence result agrees with the results of Storti and Reinhall [41] in the

limit of $\alpha \rightarrow 1$ where the fractional-coupling reduces to velocity-coupling. For this velocity-coupling case it is known that an out-of-phase motion will exist for a coupling coefficient less than 0.5 which is the result we recover in our analysis. At this critical coupling coefficient the out-of-phase limit cycle is created or destroyed in a Hopf bifurcation. The perturbation analysis indicates this as we see that the limit amplitude grows from an initial amplitude of zero. It is also known that the out-of-phase motion will only exist in the position-coupling case for a coupling coefficient greater than $-0.5/\epsilon$. In this case the out-of-phase motion loses stability in an infinite period bifurcation. This bifurcation is not detected by the perturbation method since a coupling coefficient of $O(1/\epsilon)$ is beyond its region of validity.

Next we seek to determine the stability of the out-of-phase mode in the parameter region of existence. The stability will again be studied through the corresponding variational equations and we begin by introducing the small deviations $\phi = x - q$ and $\psi = -y - q$ where $q(t)$ is the out-of-phase mode. Substituting these expressions into the coupled van der Pol equations (6.5)-(6.6) and ignoring nonlinear terms yields:

$$\phi'' - \epsilon(1 - q^2)\phi' + (1 + 2\epsilon q q')\phi = -\epsilon\gamma D^\alpha(\psi + \phi) \quad (6.58)$$

$$\psi'' - \epsilon(1 - q^2)\psi' + (1 + 2\epsilon q q')\psi = -\epsilon\gamma D^\alpha(\phi + \psi) \quad (6.59)$$

Defining the quantities $w = \phi + \psi$ and $v = \phi - \psi$ uncouples the equations.

$$w'' - \epsilon(1 - q^2) w' + (1 + \epsilon 2 q q') w = -2\epsilon\gamma D^\alpha w \quad (6.60)$$

$$v'' - \epsilon(1 - q^2) v' + (1 + \epsilon 2 q q') v = 0 \quad (6.61)$$

Observe that (6.60) is also the variational equation corresponding to (6.39), which is the equation that the out-of-phase mode satisfies. The equation on w therefore represents small deviations in the out-of-phase plane $x = -y$. We can determine if these w type deviations will give rise to instability from the previous two variable analysis by considering the stability of the fixed points of (6.54). Let δR be a small deviation from R_* where R_* is the fixed point of (6.54). Substituting $R = R_* + \delta R$ into (6.54) and Tayloring the expression with respect to δR about zero yields:

$$\delta R' = -\frac{3R_*^2 + 8\gamma \sin \frac{\alpha\pi}{2} - 4}{8} \delta R + O(\delta R^2) \quad (6.62)$$

The fixed point R_* satisfies (6.56) which reduces (6.62) to the form:

$$\delta R' = -\frac{R_*^2}{4} \delta R + O(\delta R^2) \quad (6.63)$$

The fixed points of the slow flow are therefore asymptotically stable and deviations that lie on the out-of-phase plane will not cause the out-of-phase mode to become unstable.

Returning now to the v variational equation, (6.61), we perform a two variable expansion to determine if deviations transverse to the plane of the out-of-phase mode will cause instability. Again we begin by defining:

$$\xi = \omega t, \quad \eta = \epsilon t \quad (6.64)$$

where ω is the power series expansion:

$$\omega = 1 + O(\epsilon^2) \quad (6.65)$$

By the chain rule v' and v'' become:

$$v' = \omega v_\xi + \epsilon v_\eta \quad (6.66)$$

$$v'' = \omega^2 v_{\xi\xi} + 2\omega\epsilon v_{\xi\eta} + \epsilon^2 v_{\eta\eta} \quad (6.67)$$

We posit a power series solution for v .

$$v(\xi, \eta) = v_0(\xi, \eta) + \epsilon v_1(\xi, \eta) + O(\epsilon^2) \quad (6.68)$$

The out-of-phase mode q is approximated as the limit cycle found in the previous two variable perturbation method on (6.39).

$$q = R(\eta) \cos(t - \psi(\eta)) \quad (6.69)$$

$$= \left(\left(4 - 8\gamma \sin \frac{\alpha\pi}{2} \right)^{1/2} + O(\epsilon) \right) \cos \left(t - \epsilon\gamma \cos \frac{\alpha\pi}{2} t + O(\epsilon^2) \right) \quad (6.70)$$

$$= \left(4 - 8\gamma \sin \frac{\alpha\pi}{2} \right)^{1/2} \cos t + O(\epsilon) \quad (6.71)$$

$$q^2 = R^2(\eta) \cos^2(t - \psi(\eta)) \quad (6.72)$$

$$= \left(4 - 8\gamma \sin \frac{\alpha\pi}{2} + O(\epsilon)\right) \cos^2\left(t - \epsilon\gamma \cos \frac{\alpha\pi}{2}t + O(\epsilon^2)\right) \quad (6.73)$$

$$= \left(2 - 4\gamma \sin \frac{\alpha\pi}{2} + O(\epsilon)\right) (1 + \cos(2t + O(\epsilon))) \quad (6.74)$$

$$= \left(2 - 4\gamma \sin \frac{\alpha\pi}{2}\right) (1 + \cos 2t) + O(\epsilon) \quad (6.75)$$

Substituting (6.66)-(6.75) into the v variational equation (6.61) and collecting terms we obtain:

$$O(1) : \mathcal{L}v_0 = 0 \quad (6.76)$$

$$O(\epsilon) : \mathcal{L}v_1 = \left(1 + 8\gamma \sin \frac{\alpha\pi}{2} \cos^2 t - 4 \cos^2 t\right) v_{0_\xi} - 2 v_{0_{\eta\xi}} + \left(4 - 8\gamma \sin \frac{\alpha\pi}{2}\right) \cos t \sin t v_0 \quad (6.77)$$

Where \mathcal{L} is the linear operator, $\mathcal{L}v_0 = v_{0_\xi} + v_0$. The general solution to (6.46) is given by:

$$v_0 = A(\eta) \cos \xi + B(\eta) \sin \xi \quad (6.78)$$

Substituting this general solution into the $O(\epsilon)$ equation (6.47) and grouping and identifying nonresonant terms as NRT:

$$\mathcal{L}v_1 = \sin \xi \left(2 A' - 4\gamma \sin \frac{\alpha\pi}{2} A + A\right) + \cos \xi \left(-2 B' + 4\gamma \sin \frac{\alpha\pi}{2} B - B\right) + NRT \quad (6.79)$$

The resonant terms are set to zero to obtain the slow flow equations.

$$A' = \frac{A}{2} \left(4\gamma \sin \frac{\alpha\pi}{2} - 1 \right) \quad (6.80)$$

$$B' = \frac{B}{2} \left(4\gamma \sin \frac{\alpha\pi}{2} - 1 \right) \quad (6.81)$$

From the slow flow we see that there is only one criterion for system stability:

$$\sin \frac{\alpha\pi}{2} < \frac{1}{4\gamma} \quad (6.82)$$

In Fig.6.4 the upper curve divides the parameter plane into regions where the out-of-phase mode exists and regions where it does not exist as given by $\sin \frac{\alpha\pi}{2} = \frac{1}{2\gamma}$ cf. eq.(6.57) and was previously shown in Fig.6.3. The lower curve of Fig.6.4 divides the region where the out-of-phase mode exists into stable and unstable regions and is given by $\sin \frac{\alpha\pi}{2} = \frac{1}{4\gamma}$ cf. eq.(6.82).

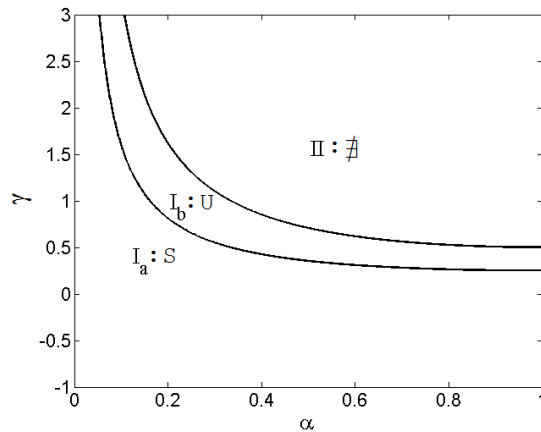


Figure 6.4: The perturbation method predicts the out-of-phase motion to be stable in region Ia and unstable in region Ib cf. eq.(6.82) . The out-of-phase motion does not exist in region II cf. eq.(6.57). S is stable, U is unstable and # is does not exist.

The perturbation method's results are again compared with numerics through the use of Matlab's ode45 routine. The results of repeated integration of (6.61) with q

given by (6.71), $\epsilon = 0.1$, and for a large number of discrete α, γ parameter pairs are shown in Fig.6.5. The asterisks represent stable parameter values and the circles unstable. The numerics are in good agreement with our perturbation method's results.

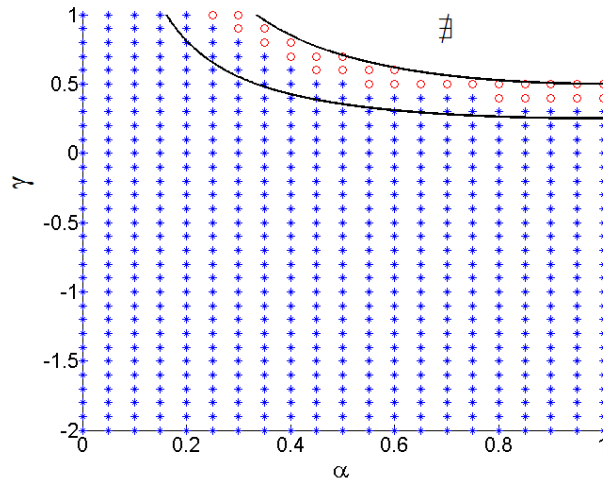


Figure 6.5: Comparison of the out-of-phase perturbation method's results with numerical integration of (6.61) with q given by (6.71) and $\epsilon = 0.1$. The asterisks represent stable parameter values and the circles unstable. \nexists represents that the out-of-phase mode does not exist.

Comparing our results again with those of Storti and Reinhall [41] in the limiting cases of $\alpha = 0$ and $\alpha = 1$ we find good agreement. For $\alpha = 0$ we find the out-of-phase mode to be stable for all values of the coupling coefficient in the region of validity of our perturbation method. This agrees with [41] as they find the out-of-phase mode to be stable for all parameter values greater than $0.5/\epsilon$ which is beyond the scope of our perturbation method. For the case of $\alpha = 1$ as the coupling coefficient is decreased from a value larger than 0.5 to a negative value, Storti and Reinhall [41] find that the out-of-phase mode transitions from not existing to being unstable and then finally stable. This transition trend is also seen in our results.

6.3 Summary

A system of two van der Pol oscillators connected through fractional-coupling was investigated in this chapter. There exists an in-phase mode and an out-of-phase mode respectively defined by $x = y$ and $x = -y$. To determine the stability of a given mode we looked at small disturbances from it. The variational equations govern the evolution of these small disturbances. We performed a two variable perturbation method on the variational equations to determine if these small disturbances would grow or decay implying then that the mode is respectively unstable or stable.

Each mode had a corresponding set of variational equations composed of one equation governing disturbances in the plane of the mode and a second equation governing disturbances transverse to the plane of the mode. For both the in-phase and out-of-phase modes' instability was seen to only be caused by disturbances transverse to the plane.

The stability results for both modes are plotted in the α, γ parameter plane, Figure 6.6. These transition curves were obtained from the two variable perturbation method and were shown to be in good agreement with numerical integration. Additionally we have reconciled our results with those of [41] in the limiting cases of $\alpha = 0$ and $\alpha = 1$ where the fractional coupling reduces to position-coupling and velocity-coupling respectively. Our work predicts that for all values of $0 \leq \alpha \leq 1$ there will be at least one region of bi-stability in the parameter plane meaning that both the in-phase and out-of-phase modes will be stable and the asymptotic behavior would then depend on initial conditions.

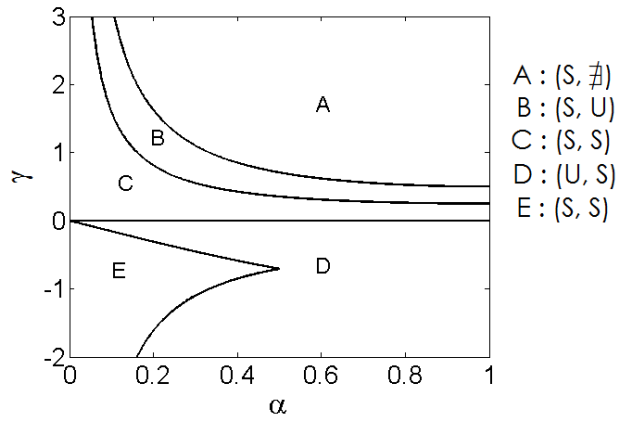


Figure 6.6: Stability results for both the in-phase and out-of-phase modes. In region A the in-phase mode is stable and the out-of phase mode does not exist as denoted by $(S, \#)$. In region B the in-phase mode is stable and the out-of-phase mode is unstable, (S, U) . In region C both the in-phase and out-of-phase modes are stable, (S, S) . In region D the in-phase mode is unstable and the out-of-phase mode is stable, (U, S) . In region E both modes are again stable, (S, S) .

CHAPTER 7

SUMMARY

In this thesis three problems in nonlinear dynamics on the topics of time delay, fractionality and synchronization were considered. Introducing a delayed quantity or a fractional derivative into a system creates a dependency on the time history of a function. This work as a whole concerns the effects of time history dependent functions on steady state behavior.

In Chapter 3 a van der Pol type system under delayed feedback with delay amplitudes of $O(1)$ and delay lags not necessarily small was studied:

$$\ddot{x} + x - \epsilon\gamma\dot{x} + \epsilon\alpha x^2\dot{x} = \beta\dot{x}(t - T) + \delta x(t - T) \quad (7.1)$$

A two variable perturbation scheme was adapted to the delayed equation by perturbing about a critical value of delay. The perturbation method yielded two Hopf bifurcation curves, which were verified numerically. These two Hopf curves bound a region of no oscillation, see Figs. 3.4-3.6. To actively quench an oscillation the delay lag may be varied to as to enter the region bounded by the Hopf bifurcation curves. Delay may therefore be used as a means to control and quench undesirable limit cycle oscillations.

The fractional Mathieu equation was investigated in Chapter 5:

$$x'' + (\delta + \epsilon \cos t)x + cD^\alpha x = 0 \quad (7.2)$$

The method of harmonic balance was applied to obtain explicit approximate expressions for the $n = 1$ and $n = 0$ transition curves separating regions of stability from regions of instability. It was found that both the shape and location of the

$n = 1$ transition curve is altered as the value of the order of the fractional derivative, α , is varied. Additionally it was shown that the minimum quantity of forcing amplitude ϵ necessary to produce instability was greatest for $\alpha^* \approx 0.735$.

A system of two van der Pol oscillators connected through fractional-coupling was studied in Chapter 3, with the stability of the in-phase and out-of-phase modes being of primary interest. The stability of a given mode was determined by analyzing the corresponding variational equations, since the variational equations govern the evolution of a small disturbances from the mode of interest. The two variable perturbation method was employed on the variational equations to determine if these small disturbances would grow or decay implying then that the mode is respectively unstable or stable. In both cases it was found that only the disturbances transverse to the plane of the mode cause instability. The two variable perturbation generates transition curves in the α, γ parameter plane which separate regions of stability from instability. The results of the two variable perturbation were checked against numerics and shown to be in good agreement. The work predicts at least one region of bi-stability in the parameter plane for all values of $0 \leq \alpha \leq 1$. The asymptotic behavior in these regions of bi-stability will be dependent on initial conditions.

APPENDIX A
MATLAB AND MAXIMA SCRIPTS

A.1 Laplace transform method results of section 4.2.1

```
function laplace_compute
clear;
clc;
close all;
global m
s = [0:.1:10];
m = length(s);
r2 = exp(i*pi/3);
r3 = exp(-i*pi/3);
x1 = exp(s).*(2/sqrt(pi)*erf_s(s.^(1/2))-1);
x2 = r2.*exp(r2^2*s).*(2/sqrt(pi)*erf_s(r2*s.^(1/2))+1);
x3 = r3.*exp(r3^2*s).*(2/sqrt(pi).*erf_s(r3*s.^(1/2))+1);
x = -1/3*(x1+x2+x3);
figure(1)
plot(s, x)

function f = erf_s(x)
global m
n = 200;
z = zeros(n, m);
for j = 0:n-1;
```

```

z(j+1, :) = x.^(2*j+1)*(-1)^j/((2*j+1)*factorial(j));
end
f = sum(z);

```

A.2 Power series method results of section 4.2.2

using macsyma as outlined below.

```

kill(all);
xs(p):=sum(x(n)*t^(n/2), n, 0, p);
xsdd(p):=diff(xs(p), t, 2);
dhx(p):=sum(gamma(n/2+1)/gamma(n/2+1/2)*x(n)*t^((n-1)/2), n, 0, p);
deq:expand(xsdd(100)+dhx(100)=0);
peq(c):=coeff(deq, t^(c/2));
x0:x(0)=0;
x1:x(1)=0;
x2:x(2)=1;
xc:[x0, x1, x2];
so(j):=solve(peq(j), x(j+4));
so(-1);
x3:%, x0;
xc:append(xc, %);
x4:x(4)=0;
xc:append(xc, [x4]);
for k:1 thru 96 do xc:append(xc, so(k));

```

```

xf:xs(100);
for i:1 thru 101 do xf:ev(xf, part(xc, 102-i));
xf;
grind(%);

```

A.3 Numerical integration code of section 4.2.3

```

function numerics
a = 1/2;
tend = 100;
h = .01;
n = tend/h;
t = zeros(1, n+1);
x = zeros(1, n+1);
y = zeros(1, n+1);
dax = zeros(1, n+1);
% t=0, m=1
x(1) = 0;
y(1)= 1;
% t=h, m=2
t(2) = h;
x(2) = x(1) + h*y(1);
y(2) = y(1);
dax(2) = 1/gamma(1-a)*(h^(-a)*(x(2)-x(1)));

```

```

% t=2h, m=3
t(3) = 2*h;
x(3) = x(2) + h*y(2);
y(3) = y(2) - h*dax(2);
m1 = [h^(-a), (2*h)^(-a)];
m2 = [y(2), y(1)];
dax(3) = 1/gamma(1-a)*(h^(-a)*(x(3)-x(2))+h/2*dot(m1,m2));
for m = 4:n+1;
    t(m) = t(m-1) + h;
    x(m) = x(m-1) + h*y(m-1);
    y(m) = y(m-1) - h*dax(m-1);
    m1 = [m1(1:m-3), 2*((m-2)*h)^(-a), ((m-1)*h)^(-a)];
    m2 = [y(m-1), m2];
    dax(m) = 1/gamma(1-a)*(h^(-a)*(x(m)-x(m-1))+h/2*dot(m1, m2));
end
plot(t, v);

```

BIBLIOGRAPHY

- [1] Ahmad, W.M. and Sprott, J.C., “Chaos in Fractional-Order Autonomous Non-linear Systems”, *Chaos, Solitons Fractals*, 16:339-351, 2003.
- [2] Atay F.M. ‘Van der Pol’s oscillator under delayed feedback’, *Journal of Sound and Vibration*, 218(2):333-339 (1998).
- [3] Barbosa, R.S., Machado, J.A.T., Vinagre, B.M. and Calderon, A.J., “Analysis of the van der pol oscillator containing derivatives of fractional order”, *J. Vibration and Control* 13:1291-1301, 2007.
- [4] Bellman R., Cooke K.L., *Differential Difference Equations*, Academic press (1963).
- [5] Bridge, J., Rand, R. and Sah. S.M., “Slow Passage Through Multiple Parametric Resonance Tongues”, *J. Vibration and Control* 15:1581-1600, 2009.
- [6] Cao, J., Ma, C., Xie, H. and Jiang, Z., “Nonlinear dynamics of duffing system with fractional order damping”, DETC2009-86401, proceedings of ASME IDETC/CIE 2009 conference, Aug.30-Sept.2, 2009, San Diego, CA.
- [7] Chen, J.H. and Chen, W.C., “Chaotic dynamics of the fractionally damped van der pol equation”, *Chaos, Solitons & Fractals* 35:188-198, 2008.
- [8] Cole J.D. *Perturbation Methods in Applied Math*, Blaisdell (1968).
- [9] Das S.L., Chatterjee A. ‘Multiple scales without center manifold reductions for delay differential equations near Hopf bifurcations’ *Nonlinear Dynamics*, 30:323-325 (2002).
- [10] Das S.L., Chatterjee A., ‘Second order multiple scales for oscillators with large delay’, *Nonlinear Dynamics*, 39:375-394 (2005).
- [11] Diethelm, K., Ford, N.J. and Freed A.D., “A predictor-corrector approach for the numerical solution of fractional differential equations”, *Nonlinear Dynamics* 29:3-22 (2002).
- [12] Galucio, A.C., Deu, J.F. and Ohayon, R., “Finite element formulation of viscoelastic sandwich beams using fractional derivative operators”, *Computational Mechanics* 33:282-291, 2004.

- [13] Ge, Z.M. and Yi, C.X., “Chaos in a nonlinear damped mathieu system”, *Chaos, Solitons & Fractals* 32:42-61, 2007.
- [14] Jesus I.S. and Tenreiro Machado J.A., “Implementation of fractional-order electromagnetic potential through a genetic algorithm”, *Commun Nonlinear Sci Numer Simul* 14:838-843, 2009.
- [15] Kilbas A.A., Srivastava H.M. and Trujillo J.J., *Theory and applications of fractional differential equations*, Elsevier, Amsterdam 2006.
- [16] Lavoie, J.L., Osler, T.J. and Tremblay R., “Fractional derivatives and special functions’, *SIAM Review* 18:240-268 (1976).
- [17] Maccari A., ‘Vibration amplitude control for a van der Pol-Duffing oscillator with time delay’, *Journal of Sound and Vibration*, 317:20-29 (2008).
- [18] Mainardi, F., “Fractional relaxation-oscillation and fractional diffusion-wave phenomena”, *Chaos, Solitons & Fractals* 7:1461-1477, 1996.
- [19] Meral, F.C., Royston, T.J. and Magin, R., “Fractional calculus in viscoelasticity: An experimental study”, *Commun Nonlinear Sci Numer Simul* 15:939-945, 2010.
- [20] Miller K. and Ross, B. *An Introduction to the Fractional Calculus and Fractional Differential Equations*, Wiley, New York, 1993.
- [21] Morrison, T.M. and Rand, R.H. “2:1 Resonance in the Delayed Nonlinear Mathieu Equation”, *Nonlinear Dynamics* 50:341-352, 2007.
- [22] Naber, M., “Linear fractionally damped oscillator” *International Journal of Differential Equations*, vol. 2010, Article ID 197020, 12 pages, 2010. doi:10.1155/2010/197020, 2010.
- [23] Nasuno, H. and Nobuyuki, S. “Power time numerical integration algorithm for nonlinear fractional differential equations”, *J. Vibration and Control* 14:1313-1332 (2008).
- [24] Nayfeh A.H. “Order reduction of retarded nonlinear systems - the method of multiple scales versus center-manifold reduction”, *Nonlinear Dynamics*, 51:483-500 (2008).

- [25] Oldham, K.B. and Spanier, J. *The Fractional Calculus*, Academic Press, New York, 1974.
- [26] Osler, T.J., "The Fractional Derivative of a Composite Function", *SIAM J. Math Anal*, 1:287-291, May 1970.
- [27] Petras, I, "A note on the fractional-order Volta's system", *Commun Nonlinear Sci Numer Simul* 15:384-393, 2010.
- [28] Podlubny, I. *Fractional Differential Equations*, Academic Press, San Diego, 1990.
- [29] Rand, R.H. and Holmes, P.J., "Bifurcation of Periodic Motions in Two Weakly Coupled van der Pol Oscillators", *Int. J. Nonlinear Mech.* 15:387-399, 1980.
- [30] Rand, R.H., "Dynamics of a Nonlinear Parametrically-Excited PDE: 2-Term Truncation", *Mechanics Research Communications* 23: 283-289, 1996.
- [31] Rand, R.H., *Lecture Notes on Nonlinear Vibrations (version 52)*, available online at <http://audiophile.tam.cornell.edu/randdocs> , 2007.
- [32] Rand, R.H. and Verdugo, A., 'Hopf bifurcation formula for first order differential-delay equations', *Communications in Nonlinear Science and Numerical Simulation*, 12:859-864, 2007.
- [33] Rand, R.H., Sah, S.M. and Suchorsky, M.K., "Fractional Mathieu equation", *Communications in Nonlinear Science and Numerical Simulation*, 15:3254-3262, 2010.
- [34] Rand, R.H., Chapter 3 in "Complex Systems: Fractionality, Time-delay and Synchronization", A.C.J. Luo and J-Q Sun, eds., pp 83-117, Springer 2011.
- [35] Rasband, S.N., *Chaotic Dynamics of Nonlinear Systems* John Wiley and Sons, Inc., 1990.
- [36] Ross, B., "A brief history and exposition of the fundamental theory of fractional calculus", in *Fractional Calculus and its Applications*, Springer Lecture Notes in Mathematics, vol.457, pp.1-36, 1975.
- [37] Rudinger, F., "Tuned mass damper with fractional derivative damping", *Engineering Structures* 28:1774-1779, 2006.

- [38] Ryabov, Y.E. and Puzenko, A., “Damped oscillation in view of the fractional oscillator equation”, *Phys Rev B* 66:184201, 2002.
- [39] Samko, S.G., Kilbas, A.A., and Marichev, O.I., *Fractional Integrals and Derivatives: Theory and Applications*, Gordon and Breach, Amsterdam, 1993.
- [40] Stoker, J.J., *Nonlinear Vibrations in Mechanical and Electrical Systems*, Wiley, New York, 1950.
- [41] Storti, D.W. and Reinhall, P.G., ”Stability of in-phase and out-of-phase modes for a pair of linearly coupled van der Pol oscillators”, *Nonlinear Dynamics The Richard Rand 50th Anniversary Volume* A.Guran, ed. World Scientific pp. 1-23 (1997).
- [42] Strogatz, S.H., *Nonlinear Dynamics and Chaos* Addison-Wesley (1994).
- [43] Suchorsky, M., Sah, S. and Rand, R., “Using delay to quench undesirable vibrations”, *Nonlinear Dynamics* 62:407-416 (2010).
- [44] Suchorsky, M., Sah, S. and Rand, R., “A pair of van der Pol oscillators coupled by fractional derivatives”, accepted for publication in *Nonlinear Dynamics*, to appear 2012.
- [45] Tavazoei, M.S., Haeri, M., Attari, M., Bolouki, S. and Siami, M., “More details on analysis of fractional-order van der pol oscillator”, *J. Vibration and Control* 15:803-819, 2009.
- [46] Torvik, P.J. and Bagley, R.L. “On the appearance of the fractional derivative in the behavior of real materials”, *Journal of Applied Mechanics* 51:294-298, 1984.
- [47] Wahl, P. and Chatterjee, A., “Averaging oscillations with small fractional damping and delayed terms”, *Nonlinear Dynamics* 38:3-22, 2004.
- [48] Wirkus S., Rand R.H. ‘The dynamics of two coupled van der Pol oscillators with delay coupling’, *Nonlinear Dynamics*, 30:205-221 (2002).
- [49] Xie, F. and Lin, X., “Asymptotic solution of the van der pol oscillator with small fractional damping”, *Physica Scripta* T136:014033, 2009.
- [50] Yonggang, K. and Xiue Zhang, “Some comparison of two fractional oscillators”, *Physica B* (article in press) doi:10.1016/j.physb.2009.08.092.

- [51] Zounes, R.S. and Rand, R.H., “Transition curves in the quasiperiodic mathieu equation”, *SIAM J.Appl.Math.* 58:1094-1115, 1998.